CRREL REPORT 90-1

DTIC FILE COPY

# Simulation of Oil Slick Transport in Great Lakes Connecting Channels

## Theory and Model Formulation

Hung Tao Shen, Poojitha D. Yapa and Mark E. Petroski February 1990

AD-A222 446

DTIC ELECTE JUN 0 5 1990 S D

DISTRIBUTION STATEMENT A
Approved for public release;
Distribution Unlimited

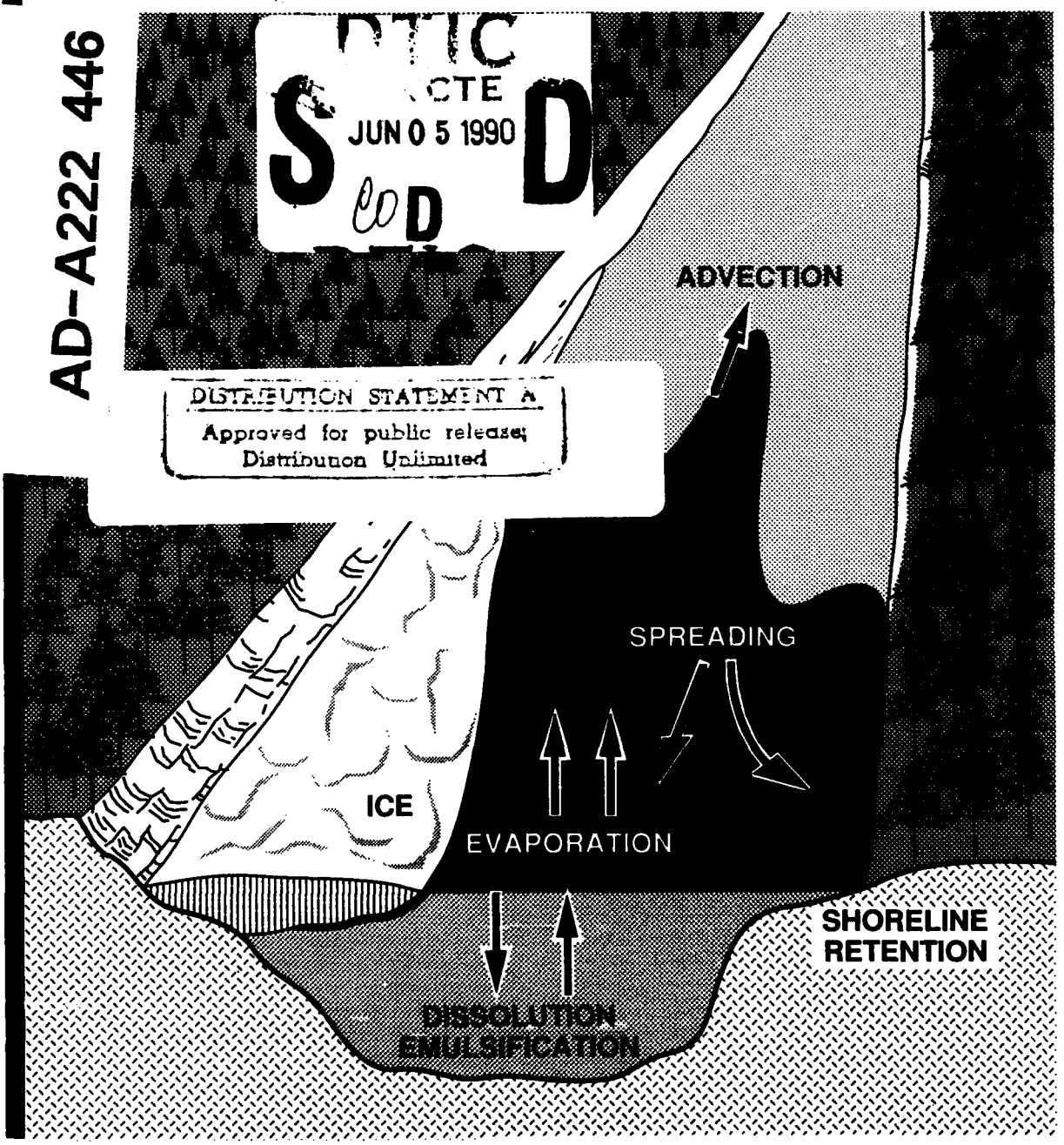


90 06 04 160

*For conversion of SI metric units to U.S./British customary units of measurement consult ASTM Standard E380,* Metric Practice Guide, *published by the American Society for Testing and Materials, 1916 Race St., Philadelphia, Pa. 19103.*

*Cover: Interaction of chemical and physical processes affecting oil spills.*

CRREL Report 90-1

**U.S. Army Corps of Engineers**
Cold Regions Research & Engineering Laboratory

# Simulation of Oil Slick Transport in Great Lakes Connecting Channels

## Theory and Model Formulation

Hung Tao Shen, Poojitha D. Yapa and Mark E. Petroski

February 1990

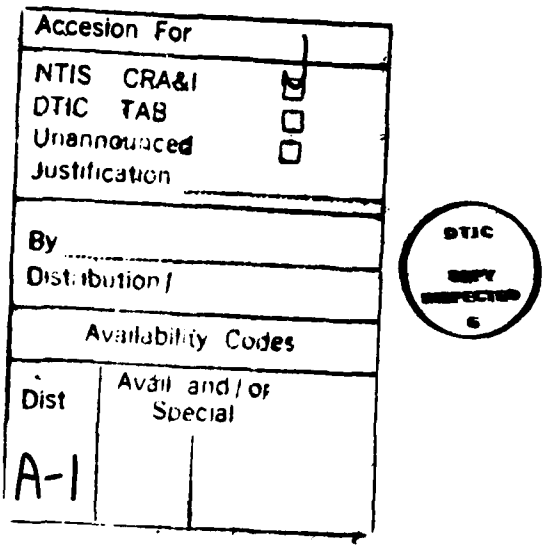


Prepared for
U.S. ARMY ENGINEER DISTRICT, DETROIT

Approved for public release; distribution is unlimited.

## PREFACE

This report was prepared by Hung Tao Shen, Professor of Civil and Environmental Engineering; Poojitha D. Yapa, Assistant Professor of Civil and Environmental Engineering; and Mark E. Petroski, graduate student, Clarkson University. The study was supported by the U.S. Army Corps of Engineers under Contract No. DACA33-85-C-0001. Steven F. Daly and Michael Ferrick of the U.S. Army Cold Regions Research and Engineering Laboratory are the contracting officer's technical representatives. The writers thank them, as well as Dan Thompson and Don Williams of the Detroit District, U.S. Army Corps of Engineers, for their cooperation and assistance throughout the study period.

The writers also acknowledge the assistance provided by the following individuals during various stages of this study: J.R. Weiser and R. Thomas, Detroit District, U.S. Army Corps of Engineers; F.H. Quinn and D.J. Schwab, Great Lakes Environmental Research Laboratory, NOAA; J. Galt and T. Raiser, NOAA; M. Sydor, Inland Water Directorate, Canada; G. Tsang and R.O. Ramseier, Environment Canada; D. Mackay, University of Toronto; J.A. McCorquodale, University of Windsor; and S. Venkatesh, Atmospheric Environment Service, Canada.

This report is one of a series of reports on numerical simulation of oil slicks in inland waterways. The series coordinator is Steven F. Daly, CRREL.

## CONTENTS



## ILLUSTRATIONS

## TABLES

# Simulation of Oil Slick Transport in Great Lakes Connecting Channels
## Theory and Model Formulation

HUNG TAO SHEN, POOJITHA D. YAPA AND MARK E. PETROSKI

## INTRODUCTION

In recent years there has been a growing concern over the increasing contamination of waterways and adjacent shoreline areas caused by oil spills. The Great Lakes–St. Lawrence River system (Fig. 1) is the world's largest freshwater system. Being a navigation corridor, it is subject to the risk of oil contamination (Beurket and Argiroff 1984, Argiroff and Weigum 1986). With the possibility of oil spills in the system, an adequate means is needed for analyzing or predicting the movement and spreading of oil slicks. In this study, computer simulation models were developed for oil slick transport in lakes and rivers. These models can either be used on a real-time basis to predict the movement of an oil spill to assist the clean-up or as scenario models to analyze possible impact of oil spills from navigation.


*Figure 1. Great Lakes–St. Lawrence River System.*

The programs are written in Fortran programming language to be compatible with a Fortran77 compiler. In addition, a user-friendly, menu-driven program with graphics capability was developed for the IBM-PC AT computer, so that these models can be easily used to assist the oil spill clean-up should a spill occur. This report provides a complete description of the analytical formulation of the models. The logic and structures of the computer programs and the instructions for using the models are described in separate reports (Shen et al., in prep. a, b;Yapa et al., in prep.).

**Fate of oil slicks**

To develop an oil spill model, it is necessary to understand the transformation process of an oil slick. In addition to the location, size and physical–chemical properties of the spill, the fate of an oil slick in a water body is governed by complex interrelated transport and weathering processes. Table 1 summarizes the environmental pathways of a typical crude oil spill at sea. Immediately upon entering a water body, the spilled oil spreads and forms a surface slick that covers a large area of the water surface and can be moved about by the action of winds, waves or currents. Some light hydrocarbons and some polar components begin to go into solution in the underlying water column, but most of these are lost to the atmosphere through evaporation. Evaporation of volatile components and dissolution of hydrocarbons may reduce the volume of spilled oil by as much as 50% during the first few days following the spill. In turbulent waters, some of the oil is emulsified into the water column as small dispersed droplets. These droplets may become dispersed by currents, or they may become attached to suspended particulate matter and slowly settle to the bottom. The turbulence action can also cause water to become entrained in the oil, forming water-in-oil emulsion that may eventually weather further to form dense tar balls. While all these processes are occurring, photochemical reactions and microbial biodegradation can also change the character of the oil and reduce the amount of oil present.

**Table 1. Pathways for the environmental fate of crude oil (Butler et al. 1976).**

| *Pathway* | *Time scale (days)* | *Percentage of initial oil* |
|---|---|---|
| Evaporation | 1 – 10 | 25 |
| Solution | 1 – 10 | 5 |
| Photochemical | 10 – 100 | 5 |
| Biodegradation | 50 – 500 | 30 |
| Disintegration and sinking | 100 – 1000 | 15 |
| Residue | >100 | 20 |
| Total | | 100 |

These physical and chemical processes can be categorized as advection, spreading, evaporation, dissolution, emulsification, auto-oxidation, sedimentation and biodegradation. A number of excellent reviews on these processes have been published (Stolzenbach et al. 1977, Wheeler 1978, Jordan and Payne 1980, Huang and Monastero 1982). Figure 2 is a schematic representation of the transport and weathering processes showing time periods for which each of these processes is important. It is clear that the oil undergoes significant modification during the first few hours following a spill. A brief discussion of each of these physical, chemical and biological processes follows.

*Advection*

Advection is a physical process that involves the drifting of the surface oil slick and the subsurface oil. The advection of surface oil is caused by the combined effects of surface current and wind drag. The advection of subsurface oil is the movement of the oil entrained in the flow due to the subsurface current.

*Spreading*

Spreading also involves the areal expansion of oil slicks. The spreading process includes mechanical spreading and turbulent diffusion. In mechanical spreading the area of the surface oil slick expands because of the balancing forces of inertia, gravity, viscosity and surface tension. Turbulent diffusion is the spreading of the surface oil because of the fluctuations of the wind and current velocities.

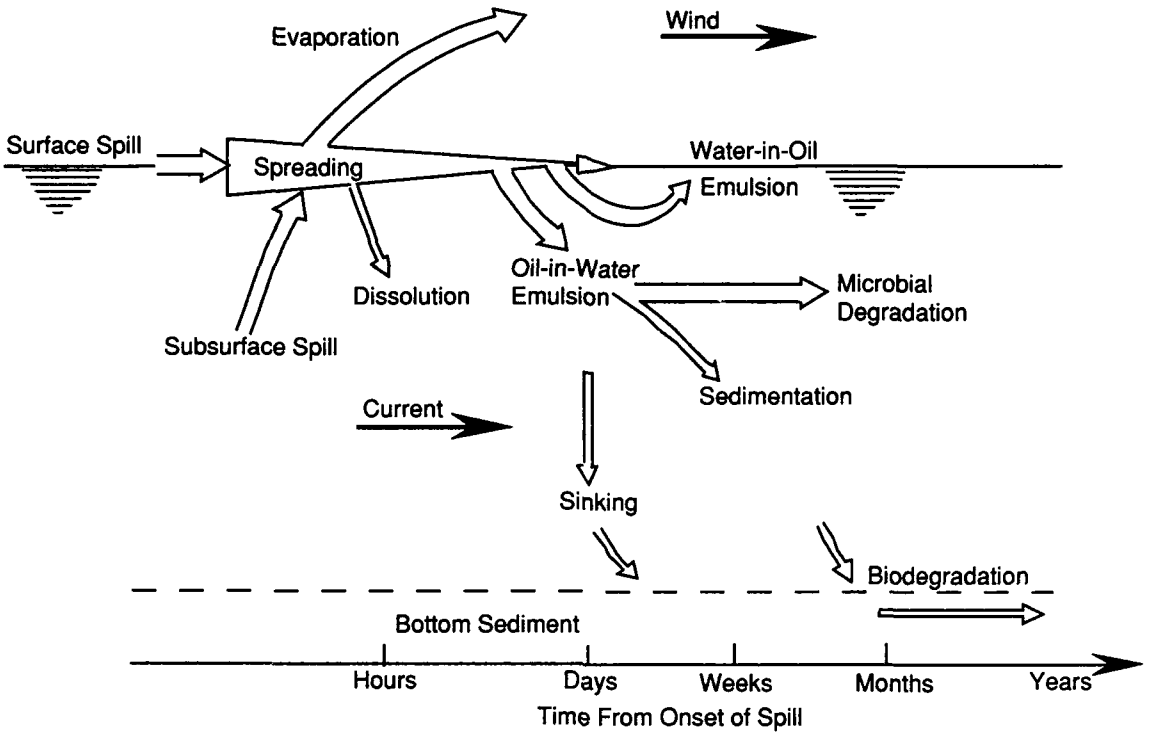


*Figure 2. Physical, chemical and biological processes affecting oil slick transformation.*

Since the spreading of oil will increase weathering processes such as evaporation, dissolution, photo-oxidation and biodegradation, it is one of the most important processes affecting the fate of the spilled oil.

*Evaporation*

Evaporation begins immediately after the spill. As the spill spreads, more of the hydrocarbons are exposed to the atmosphere, causing evaporation rates to increase. The amount and rate of evaporation depend on the percentage of light (or volatile) components in oil. Evaporation is the most significant physical–chemical process in reducing the oil volume. Highly refined oils can lose 75% or more of their volume through evaporation within days.

*Dissolution*

Some oil components will be lost from a slick by dissolving in the water column. Only the low-molecular-weight hydrocarbons have an appreciable solubility in water. The fraction of oil dissolved is very small compared to that evaporated, but this extraction process can be important because of the toxicity of the dissolved fraction.

*Emulsification*

The formation of oil-in-water emulsion is an important mode of oil dispersion. Turbulence and wave action mix the surface layer of oil into the water column by causing many very small globules of oil to form, which can be rapidly dispersed vertically into the water column where they are subject to subsurface transport. The eventual fate of oil-in-water emulsions is probably dissolution in the water column, attachment to solid particles and biodegradation. Water-in-oil emulsions can also form, particularly with heavy crudes and residual oils. The resulting emulsions, which contain a large percentage of water but have a semisolid texture, are often referred to as "chocolate mousses" because of their appearance. These emulsions may persist on the water surface and disintegrate into tar lumps after a long time if they do not wash up on the shore.

*Auto-oxidation*

In the presence of atmospheric oxygen, natural sunlight has sufficient energy to change the composition of the oil. This photo-oxidation process is very slow. The extent and rate of the photo-oxidation primarily depend on the chemical composition of the oil and its optical density. Little is known about the effect of photochemical reactions in the overall oil slick transformation process.

*Sinking and sedimentation*

Some of the spilled oil ultimately sinks if it does not wash up on the shore. This sinking and sedimentation process occurs because the density of the oil increases when the lighter fractions of the oil evaporate or dissolve or when the oil adheres to suspended sediment. This process may eventually cause oil fractions to sink to the bottom, where they may be moved laterally, they may be resuspended, or they may undergo further biological or physical–chemical reaction.

Little is known about the ultimate fate of the sedimented oil. All of the processes just described, except possibly photo-oxidation, can only redistribute the oil. They cannot remove the hydrocarbon from the environment. Real degradation takes place through biochemical oxidation; this process is the principal long-term means of removing the spilled oil from the environment.

## Oil spill simulation models

Many of the oil spill models developed during the last decade simulate only the advection and spreading processes. Other models deal extensively with physical–chemical processes but lack the component for simulating the advection of the slick. Only in recent models have the incorporation of both the transport and weathering processes been attempted (Huang and Monastero 1982). Since there are not enough data to establish a reliable analytical formulation for many of the weathering processes, it is impractical to include all of them in an oil spill simulation model. It would be more useful to include the most significant processes (i.e., those accounting for the bulk of the oil) while omitting others so that uncertainty in the outcome can be reduced. In addition, since part of the oil spilled in water bodies, especially in rivers and lakes, will be washed up on shore, appropriate shoreline boundary conditions must also be considered in a simulation model.

Almost all of the existing oil slick models were developed for coastal marine environments. Only a few models were developed for rivers and lakes (Huang and Monastero 1982). Tsahalis (1979b) developed a simulation model for predicting the transport, spreading and associated shoreline contamination of oil spills in rivers. In this model the current velocity distribution in the river is calculated by empirical relationships determined from field data, with some modifications for the secondary current in riverbends. The oil slick is assumed to remain circular, with its radius calculated according to Fay's spreading laws (Fay 1969, 1971). The drift velocity of the slick is determined by formulas derived by Tsahalis (1979) from laboratory experiments.

Fingas and Sydor (1980) developed a two-dimensional model for oil spills in rivers. In this model the current velocity distribution is determined by the two-dimensional finite-difference scheme of Leendretse (1970). The entire oil slick volume is represented by a large number of individual particles. The drift velocities of these particles are determined by the wind factor approach. A random fluctuation component is included to represent horizontal diffusion. The spreading of the oil slick is calculated by Fay's spreading laws for circular slicks. For oil spills in lakes, the only model is one developed at the Great Lakes Environmental Research Laboratory (Boyd 1979, Schwab et al. 1984) for the Great Lakes; this is basically a model for predicting the motion of a group of surface particles. The movement of an oil slick can be simulated using this model by representing the oil slick as a group of particles. None of these three models considered oil weathering processes, so the effects of weathering on the oil slick transformation cannot be accounted for.

In this study, computer models were developed for simulating the fate of oil spills in a river or lake including the effect of ice covers. None of the previous models for oil spills in rivers and lakes took this factor into consideration. The purpose of these simulation models is to assist the on-scene com-

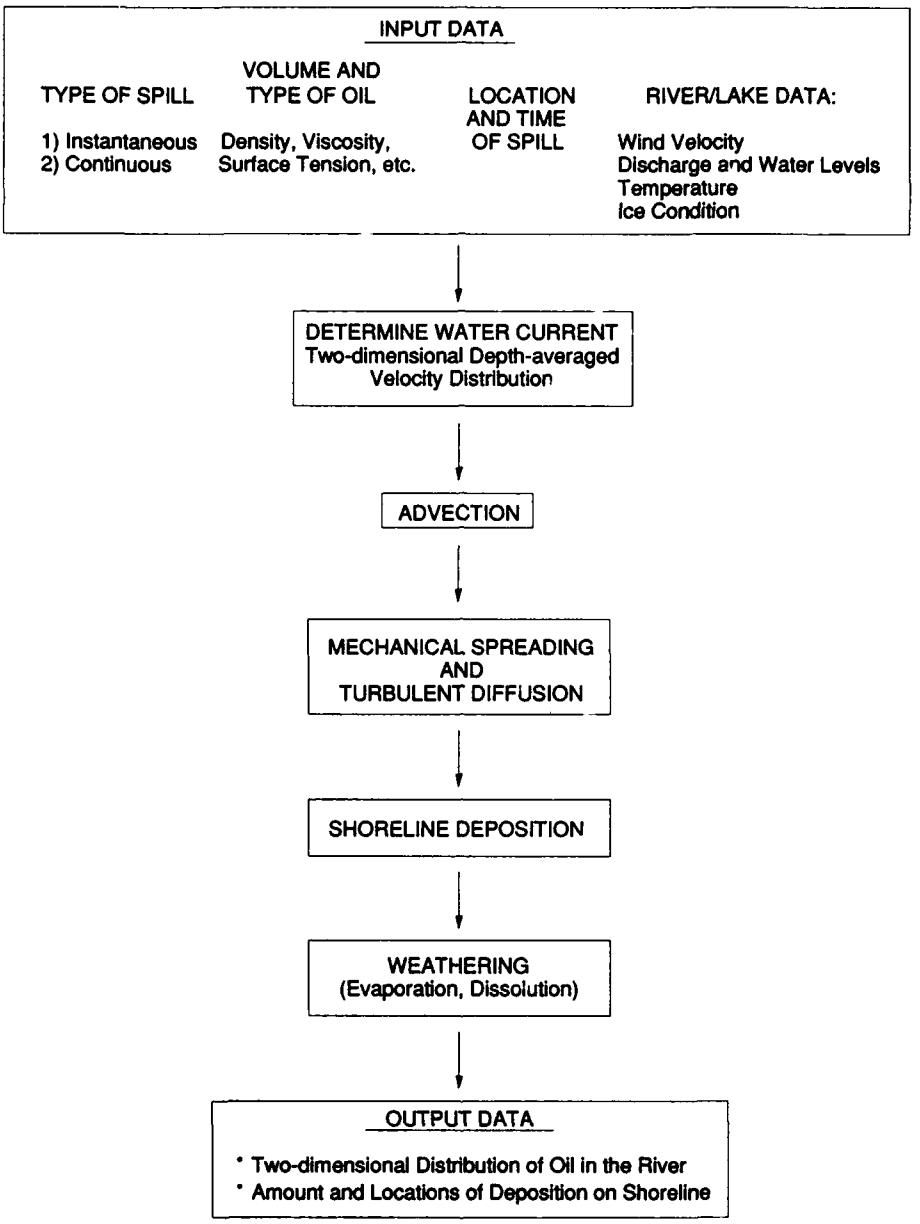


*Figure 3. Structure of the simulation model.*

mander to develop clean-up measures in the case of an actual spill and to assess likely environmental impacts of possible spills. The models are primarily designed for predicting the motion of an oil slick in rivers or lakes.

Figure 3 shows the structure of the simulation model. Detailed discussions of the model formulation will be presented later. The models developed in this investigation consider the oil slick to be composed of a large number of discrete parcels, which are tracked for their positions and volume to each time level during the period of simulation. The two-dimensional velocity distributions of the underlying river or lake water are first computed. Using the wind velocity and the computed current velocity, the model determines the advection of each parcel in the slick using the wind factor approach. The spreading of the slick is simulated by considering both the mechanical spreading and surface turbulent diffusion. The model developed by Fay (1969, 1971) is used to simulate mechanical spreading, while a random-walk simulation is used to account for the spreading due to surface turbu-

lence. The loss of oil due to shoreline deposition is calculated according to the oil retention capability of the shoreline that the oil slick reaches. The loss of oil due to evaporation and dissolution are calculated based on empirical formulations that consider the effects of slick area, wind velocity, temperature and oil properties. Since weathering processes that occur long after the onset of spill are not well understood and are less significant, these processes are not considered in the model. This is justified from the operational point of view, since the oil will be washed up on shore and clean-up measures will be [illegible] shortly after the spill.

## THEORY AND MODEL FORMULATION

### Analytical framework

The transformation of an oil slick is affected by a number of complex physical and chemical processes. To facilitate the discussion of the model formulation, an analytical framework based on the equations of motion of a surface oil slick will first be presented. For a surface oil slick, as shown in Figure 4, the two-dimensional depth-averaged equation of motion can be written as (Ahlstrom 1975, Stolzenbach et al. 1977)

$$\frac{\partial(\rho_o h)}{\partial t} + \frac{\partial(\rho_o u h)}{\partial x} + \frac{\partial(\rho_o v h)}{\partial y} = -\phi_s - \phi_b - Rh \tag{1}$$

$$\frac{\partial u}{\partial t} + u\frac{\partial u}{\partial x} + v\frac{\partial u}{\partial y} = -g\left(\frac{\rho_w - \rho_o}{\rho}\right)\frac{\partial h}{\partial x} - \frac{\tau_{bx}}{\rho h} + \frac{\tau_{sx}}{\rho h} \tag{2}$$

$$\frac{\partial v}{\partial t} + u\frac{\partial v}{\partial x} + v\frac{\partial v}{\partial y} = -g\left(\frac{\rho_w - \rho_o}{\rho}\right)\frac{\partial h}{\partial y} - \frac{\tau_{by}}{\rho h} + \frac{\tau_{sy}}{\rho h} \tag{3}$$

where $x$ and $y$ = space variables
$t$ = time
$u$ and $v$ = components of the oil velocity
$\rho_o$ and $\rho_w$ = densities of oil and water, respectively
$h$ = oil slick thickness
$g$ = acceleration due to gravity
$\tau_{bx}$ and $\tau_{by}$ = shear stress components on the bottom of the oil slick
$\tau_{sx}$ and $\tau_{sy}$ = shear stress components on the top surface of the oil slick
$\phi_s$ = rate of oil flux outward through the top surface, e.g., evaporation
$\phi_b$ = rate of oil flux outward through the bottom surface, e.g., dissolution
$R$ = other source and sink terms.

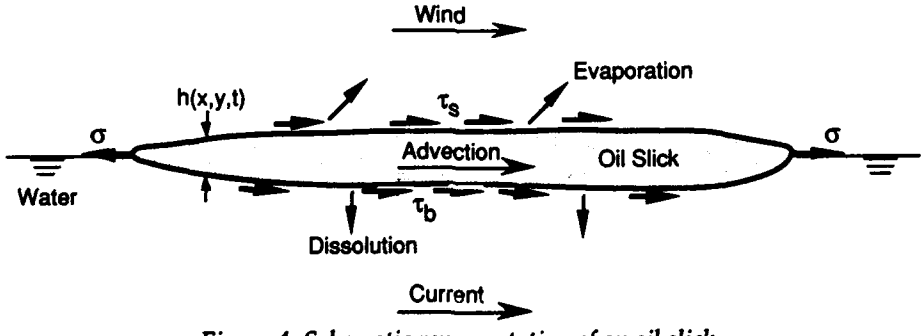


*Figure 4. Schematic representation of an oil slick.*

The density of oil can be determined from its specific gravity. Typical values of the specific gravity are 0.7 for gasoline, 0.8 for kerosene, 0.84 for diesel or no. 2 fuel oil, and 0.98 for Bunker C or no. 6 fuel. The specific gravity of crude oils varies between 0.80 and 0.99 (Bishop 1983).

The boundary condition at the circumference of the slick is that the force parallel to the water surface and normal to the slick boundary $f_n$ be balanced by the net surface tension force:

$$f_n = \sigma = \sigma_{aw} - \sigma_{oa}\cos\theta_{oa} - \sigma_{ow}\cos\theta_{ow}$$

$$\approx \sigma_{aw} - \sigma_{oa} - \sigma_{ow} \qquad (4)$$

where $\sigma_{aw}$ = surface tension of the air/water interface (72.75 dynes/cm at 20°C)
$\sigma_{oa}$ = surface tension of the air/oil surface (20 dynes/cm for many crudes)
$\sigma_{ow}$ = surface tension of the oil/water interface (varies between 15 and 25 dynes/cm)
$\theta_{oa}$, $\theta_{aw}$ = contact angles between oil and air and between oil and water (Stolzenbach et al. 1977).

Equations 1–4 clearly show that the movement of an oil slick is governed by the advection due to the viscous forces acting on the top and bottom surfaces of the slick, the spreading due to gravitational, viscous and surface tension forces, and the changes in the mass and physical–chemical properties of the oil due to various weathering processes.

A number of studies have attempted to analyze in detail the hydrodynamic problem defined above (Kerr and Babu 1970, DePietro and Cox 1979, Foda and Cox 1980). These complex mathematical treatments are not suitable for real field problems. In the present study, a Lagrangian discrete-parcel algorithm is used. In this algorithm the oil slick is viewed as a large ensemble of small parcels. Each parcel has associated with it a set of spatial coordinates and a specific quantity of mass. The movement of each parcel in the river or the lake is affected by the wind, water currents and the concentration of surrounding parcels. If a large number of parcels are released in a water body and their discrete paths and masses are followed and recorded as functions of time relative to a fixed reference grid, then the density distribution of the ensemble in the water body can be interpreted as the concentration of the oil. This approach requires an efficient bookkeeping procedure rather than the solution of a large matrix associated with a conventional Eulerian finite-difference or finite-element methods. The algorithm is inherently stable with respect to time steps, although the time step should be compatible with the grid size and velocity for numerical accuracy (Cheng et al. 1984). Since the movement of each parcel in the oil slick depends on the distribution of the entire ensemble, all parcels must be traced at each time level before proceeding to the next.

The detailed structure and implementation of the numerical model will be discussed later. In the following sections the analytical formulations for each component of the model will be discussed.

**River current simulation**

Since the water current affects both the advection and the spreading of an oil slick, the distribution of both the magnitude and the direction of the current must be determined first. There are numerous numerical methods for determining the two-dimensional flow distribution in shallow waters (Leendretse 1970, Grubert 1976, Hamilton et al. 1982). However, because of stability and accuracy problems of the numerical method, the geometric element size $A_e$ and the size of the time steps $t$ are limited by $t \leq (A_e/gh)^{1/2}$. This makes the method impractical for long rivers. In view of the need for simulating flow distributions in long river reaches, an alternative approach is taken in the present study. In the present approach, the time-dependent discharge distribution $Q(x,t)$ along the river is first obtained by using a one-dimensional hydraulic transient model,* which was developed based on the St. Venant equations:

*For example, the unsteady flow model for the Great Lakes connecting channels developed by R. Thomas of the Detroit District, U.S. Army Corps of Engineers.

$$\frac{\partial Q}{\partial x}+\frac{\partial A}{\partial t}=0 \tag{5}$$

$$\frac{\partial Q}{\partial t}-\left(\frac{Q}{A}\right)^2\frac{\partial A}{\partial x}+\frac{2Q}{A}\frac{\partial Q}{\partial x}+gA\frac{\partial H}{\partial x}-gA(S_o-S_f)=0 \tag{6}$$

where $x$ = longitudinal distance along the river
$A$ = flow cross-sectional area
$H$ = water level
$S_o$ = bed slope
$S_f$ = frictional slope.

The friction slope can be calculated by Manning's equation:

$$S_f=\frac{n_b^2Q^2}{2.21A^2R^{4/3}} \tag{7}$$

where $R$ is the hydraulic radius and $n_b$ is the Manning's roughness coefficient for the bed. For an ice-covered reach, the composite Manning's coefficient, which accounts for the resistance of ice cover and the riverbed, should be used instead of $n_b$. The composite Manning's coefficient $n$ can be calculated by the Belokon–Sabaneev formula:

$$n=\left[\frac{1}{2}\left(n_i^{3/2}+n_b^{3/2}\right)\right]^{2/3} \tag{8}$$

where $n_i$ is the Manning's roughness coefficient for the ice cover. The hydraulic radius can be assumed to be half of the flow depth for ice-covered reaches.

Once the one-dimensional solution is obtained, the discharge $Q$ can be distributed across the width of the river using a stream-tube model (Shen and Ackermann 1980) to give the two-dimensional velocity distribution at selected cross sections.

*Two-dimensional velocity distribution*

For any channel cross section, as shown in Figure 5, the transverse distribution of the flow can be determined using a simplified method developed by Shen and Ackermann (1980). In this method, the cross section is first divided into trapezoidal elements. By applying Manning's equation to the ratio of discharges between the entire cross section and a partial cross section (Fig. 5), the following

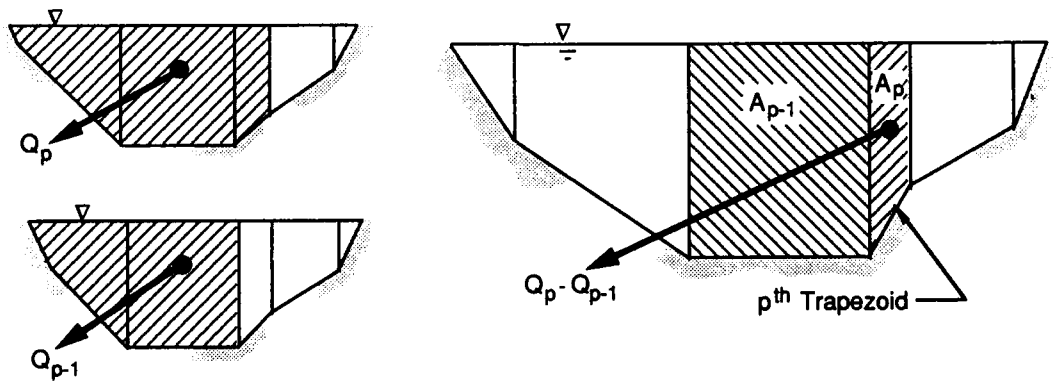


*a. Cumulative discharges over a partial cross section.*

*b. Area and discharge for the $p^{th}$ trapezoid.*

*Figure 5. Method for determining the transverse distribution of the flow for any cross section.*

expression can be written:

$$\frac{Q_P}{Q} = \frac{\sum_{p=1}^{P} A_p R_p^{2/3}}{\sum_{n=1}^{N} A_n R_n^{2/3}} \tag{9}$$

where $P$ = number of trapezoids in the partial cross section
$N$ = total number of trapezoids describing a cross section geometry
$Q_P$ = cumulative discharge up to and including the $p^{th}$ trapezoid
$Q$ = the total discharge through the entire cross section
$A_n$ and $R_n$ = area and hydraulic radius, respectively, of the $n^{th}$ trapezoid
$A_p$ and $R_p$ = area and hydraulic radius, respectively, of the $p^{th}$ trapezoid.

The cumulative discharge $Q_p$ can be computed by first rewriting eq 9 as

$$Q_P = F_Q \sum_{p=1}^{P} (A_p R_p^{2/3}) \tag{10}$$

where

$$F_Q = \frac{Q}{\sum_{n=1}^{N} (A_n R_n^{2/3})} \tag{11}$$

and

$$Q_P - Q_{P-1} = F_Q A_p R_p^{2/3}. \tag{12}$$

Based on the computed distribution of $Q_p$, stream-tube boundaries within the cross section can be determined by simple interpolation. Once the stream-tube boundaries are located, the flow through each stream tube $Q_s$ is divided by the cross-sectional area of the stream tube $A_s$ to obtain the depth-averaged velocity:

$$V_p = Q_s / A_s . \tag{13}$$

This velocity is then assigned to the center of the stream tube. Applying this procedure to successive cross sections along the river produces a two-dimensional depth-averaged velocity distribution. The directions of velocity vectors are the same as the vectors connecting center points of each stream tube at successive cross sections. As an example, the simulated depth-averaged velocity distribution for a reach of the St. Clair River is shown in Figure 6a.

Once the velocity distribution along stream tubes is established, the distribution of velocity for all the points in a predefined grid system, as shown in Figures 6b and c, can be obtained through linear interpolations. Calculated velocities compare favorably with data obtained in the field (U.S. Army Corps of Engineers, Detroit District 1974).

**Lake circulation**

The following equations of motion describe the circulation in shallow lakes, if nonlinear convective terms are neglected:

$$\frac{\partial M}{\partial t} - fN = -gD\frac{\partial H}{\partial x} + \frac{1}{\rho_w}(\tau_x^s - \tau_x^b - \tau_x^i) \tag{14}$$

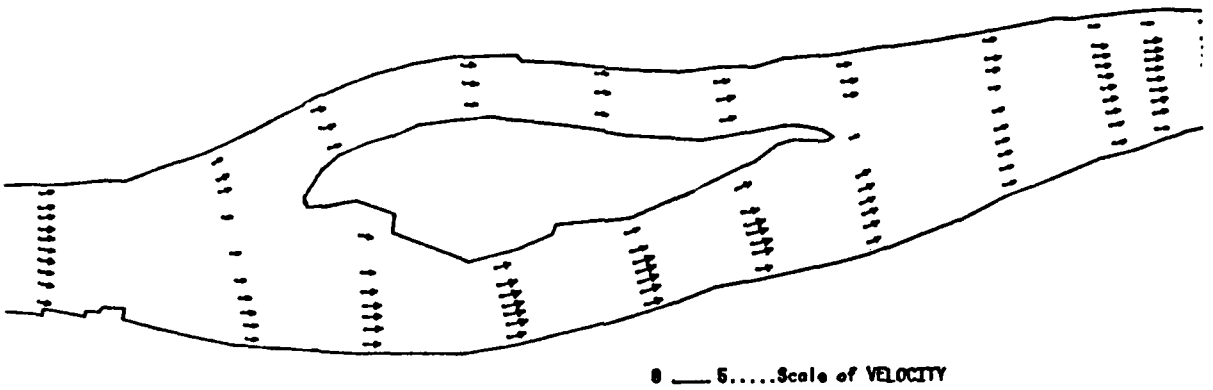


*a. Velocity distribution in stream tubes.*

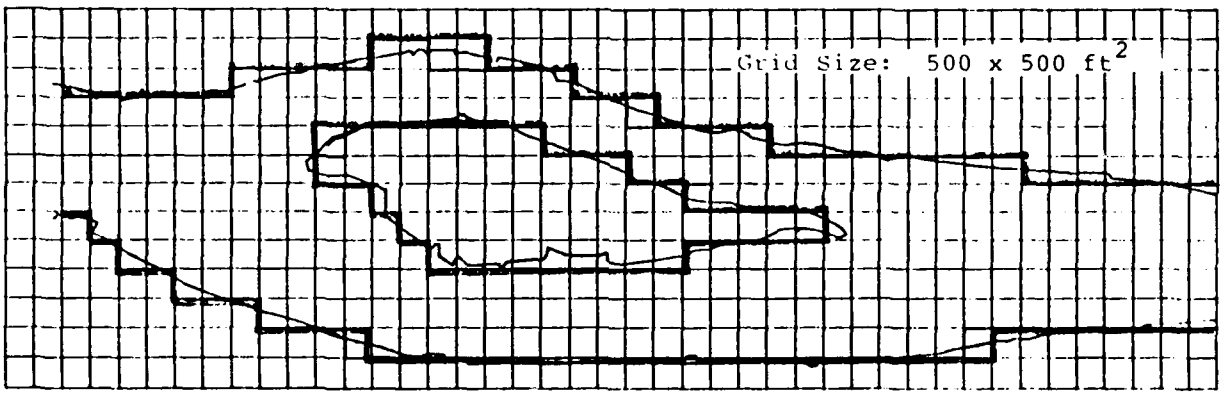


*b. Superimposed grid system.*

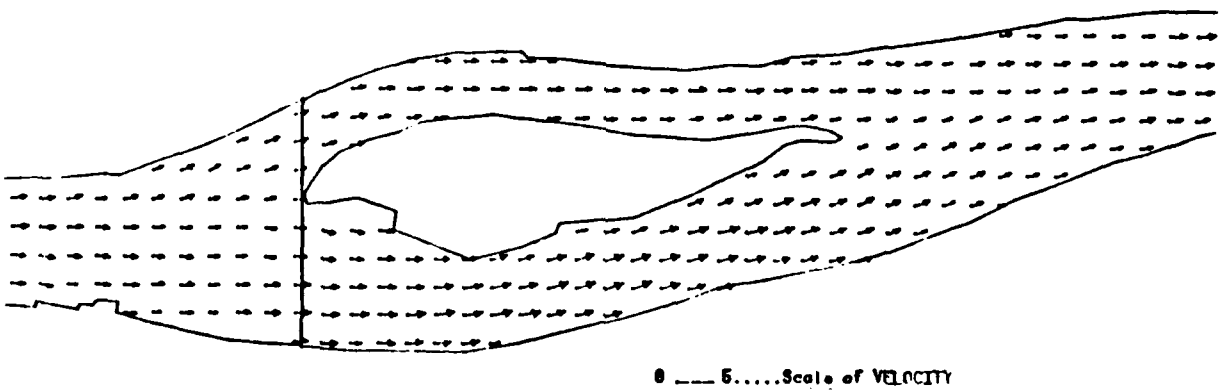


*c. Velocity distribution on the grid system.*

*Figure 6. Method for determining the velocity distribution for a typical river reach.*

$$\frac{\partial N}{\partial t} - fM = -gD\frac{\partial H}{\partial y} + \frac{1}{\rho_w}(\tau_y^s - \tau_y^b - \tau_y^i) \tag{15}$$

and

$$\frac{\partial H}{\partial t} + \frac{\partial M}{\partial x} + \frac{\partial N}{\partial y} = 0 \tag{16}$$

where $M = u_c D$

$N = v_c D$

$u_c$ and $v_c$ = depth-average velocity components

$D$ = depth of the flow

$H$ = water surface elevation
$g$ = acceleration due to gravity
$f$ = $\Omega \sin\phi$ (the coriolis parameter)
$\Omega$ = angular velocity of the earth
$\phi$ = latitude
$\tau_x^s$ and $\tau_y^s$ = components of the wind stress
$\tau_x^b$ and $\tau_y^b$ = components of the bed shear
$\tau_x^i$ and $\tau_y^i$ = components of the shear stress at the ice/water interface
$x$ and $y$ = space variables
$t$ = time.

For simulating the circulation pattern in the Lake St. Clair, the RLID finite-difference model developed by Schwab et al. (1981) is used. This model neglects the free surface fluctuation. Equation 16 then leads to the existence of the stream function $\psi$, defined by

$$M = -\frac{\partial \psi}{\partial y}, \quad N = \frac{\partial \psi}{\partial x}. \tag{17}$$

Combining this with eq 14 and 15 will yield

$$\frac{\partial}{\partial t}\left(\nabla \cdot D^{-1} \nabla \psi\right) + f\left(\frac{\partial \psi}{\partial x}\frac{\partial D^{-1}}{\partial y} - \frac{\partial \psi}{\partial y}\frac{\partial D^{-1}}{\partial x}\right) = \frac{\partial}{\partial x}\left(\frac{\tau_y^s - \tau_y^b - \tau_y^i}{D\rho_w}\right) - \frac{\partial}{\partial y}\left(\frac{\tau_x^s - \tau_x^b - \tau_x^i}{D\rho_w}\right). \tag{18}$$

Equation 18 is used to solve for $\psi$ values through a second-order finite-difference scheme. The velocity distribution is determined from the calculated $\psi$ values. Figure 7 shows sample results for the velocity distribution in Lake St. Clair.

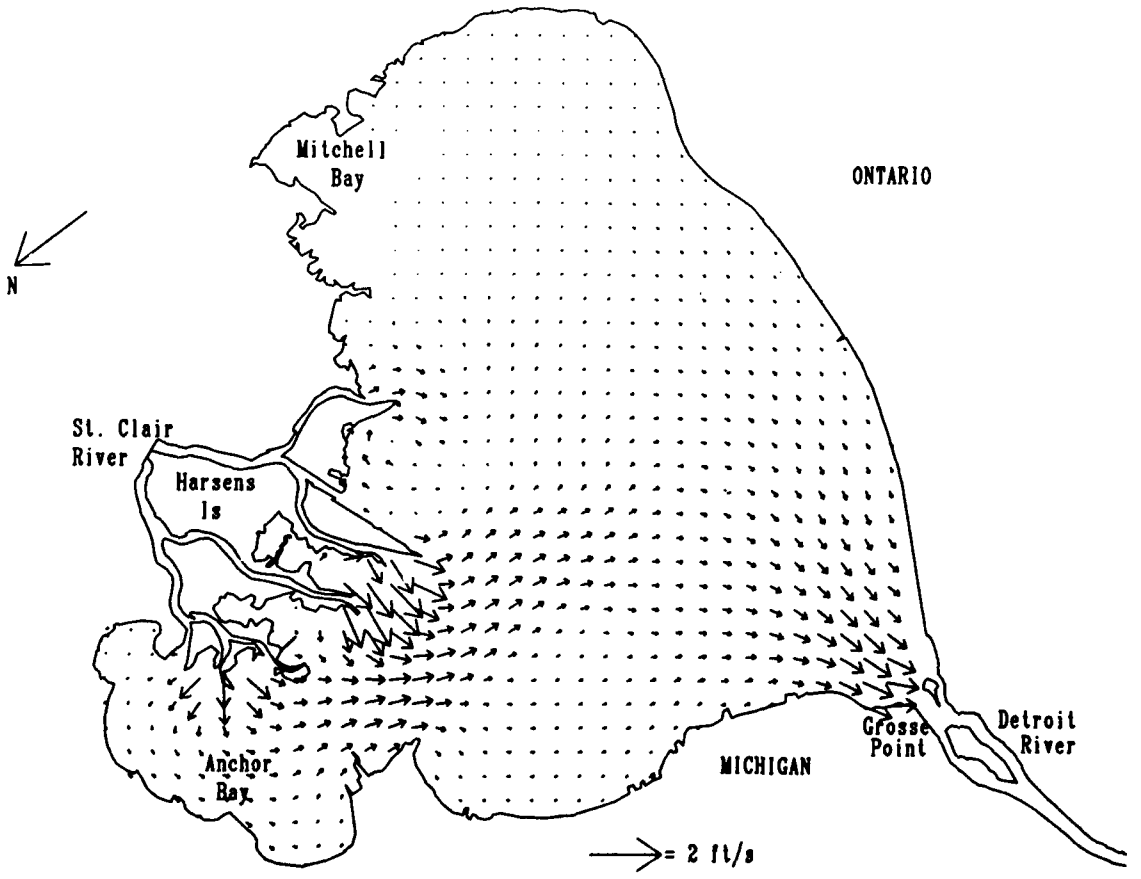


*Figure 7. Velocity distribution in Lake St. Clair. The stage and discharge at the outlet of the lake are 575.04 ft and 210,000 ft³/s, respectively.*

## Advection

*Advection in open water*

Advection or drifting of oil on the water surface is the result of the combined action of wind, current and wind-generated waves (Schwartzberg 1971, Tsahalis 1979a). The drift velocity of the surface oil is usually considered to be the vector sum of a wind-induced drift and a water-current-induced drift (Stolzenbach et al. 1977). In the present model the advective velocity of each oil parcel is computed as

$$\vec{V}_t = \vec{V} + \vec{V}' \tag{19}$$

where $\vec{V}_t$ is the drift velocity of an oil parcel and $\vec{V}$ and $\vec{V}'$ are the mean and turbulent fluctuation components of the drift velocity. The component $\vec{V}'$ is included to simulate the horizontal diffusion of the oil parcels. The formulation for $\vec{V}'$ will be discussed later in this section. The mean velocity component $\vec{V}$ includes both the wind and water current effects and can be calculated by the formula

$$\vec{V} = \alpha_w \vec{V}_w + \alpha_c \vec{V}_c \tag{20}$$

where $\vec{V}_w$ = wind velocity at 10 m above the water surface
$\vec{V}_c = u_c + \vec{V}_c$ = depth-averaged current velocity
$\alpha_w$ = factor to account for the drift of the surface slick due to wind
$\alpha_c$ = factor to account for the drift of the oil slick at the water surface due to the current.

Wind-induced surface currents have been reported to vary between 1% and 6% of the wind speed, with 3% being the most widely used drift factor in oil slick trajectory models (Stolzenbach et al. 1977). Based on Madsen's (1977) Ekman layer model, a drift factor of 0.03 can also be obtained with appropriate values of equivalent roughness height of the free surface (Huang and Monastero 1982).

If the velocity profile is assumed to be logarithmic, the surface velocity of the water current can be related to the depth-averaged current velocity by the relationship

$$\frac{V_s}{V_c} = 1 + \frac{u_*}{\kappa V_c} \tag{21}$$

where $V_s$ = surface velocity
$u_*$ = shear velocity
$\kappa$ = Karman constant (0.4).

Calculations based on conditions in the connecting channels show that the ratio $V_s/V_c$ varies between 1.1 and 1.2, with most of the values equal to 1.1. In the present simulation, values of 0.03 and 1.1 are used for $\alpha_w$ and $\alpha_c$, respectively.

*Advection under an ice cover*

Oil spills under ice have received little theoretical or laboratory treatment. As suggested by the experimental study of Cox and Schultz (1981), an ice cover may be classified into three categories when determining slick advection: the ice cover may be smooth, it may contain small roughness elements, or it may contain large roughness elements. The following discussion summarizes the results of limited experimental studies and serves as the basis for modeling the advection of oil in the present simulation.

Under smooth ice covers with no current, the oil will rest at an equilibrium thickness that is described by the empirical equation

$$\delta_{eq} = 1.67 - 8.5(\Delta\rho_w) \tag{22}$$

where $\delta_{eq}$ = static equilibrium slick thickness (cm)

$\Delta = (\rho_w - \rho_o)/\rho_w$ = relative density difference between oil and water
$\rho_w$ and $\rho_o$ = water and oil densities, respectively (g/cm).

An ice cover is considered to be smooth when the height of the ice roughness is smaller than the equilibrium thickness of the oil $\delta_{eq}$.

The depth–averaged current velocity at which the oil just begins to move along an ice cover is called the threshold velocity $U_{th}$. For a smooth cover the value of $U_{th}$ was empirically determined to be a function of the oil viscosity $\mu_o$ and is given as

$$U_{th} = 305.79/(88.68 - \mu_o) \tag{23}$$

where $U_{th}$ is in cm/sec and $\mu_o$ is in g/cm-s. Viscosities for crude and fuel oils fall in the range of 5–50 centipoises.* Typical values of oil viscosity can be found in fluid mechanics books (e.g. Rouse 1946).

A rough ice cover can retain the oil between the roughness elements. As the current velocity increases, the oil creeps along the upstream face of the roughness element until it spills over the element and moves downstream. The threshold current velocity at which the oil will move downstream under a rough ice cover is called the failure velocity $U_{fl}$:

$$U_{fl} = 1.5\left\{2\left(\frac{\rho_o+\rho_w}{\rho_o\rho_w}\right)[\sigma_{o/w}g(\rho_w-\rho_o)]^{1/2}\right\}^{1/2} \tag{24}$$

where $\sigma_{o/w}$ is the oil/water interfacial tension. The failure velocity $U_{fl}$ is the velocity above which no oil can be contained upstream of a large roughness element. If the depth-averaged current velocity is less than the threshold velocity, the slick will not advect. If the depth-averaged velocity is greater than the threshold velocity, $U_{th}$ or $U_{fl}$, the relationship between the current velocity and the slick velocity is

$$\left(1 - \frac{V}{V_c}\right)^2 = \frac{K}{0.115F_\delta^2 + 1.105} \tag{25}$$

with

$$F_\delta = \frac{V_c}{\sqrt{\Delta g \delta_{eq}}} \tag{26}$$

where $V$ = mean drift velocity
$V_c$ = current speed
$K$ = friction amplification factor
$F_\delta$ = slick densimetric Froude number
$g$ = acceleration due to gravity.

The value of $K$ is a function of the roughness height of the cover. With the limited data available, $K$ is assumed to vary linearly between 1.0 for a smooth cover and 2.6 for an ice cover with a Manning's roughness coefficient $n_i$ of 0.055.

*Horizontal diffusion*

The term $V'$ in eq 19 is included to account for horizontal diffusion caused by the turbulent fluctuation of the drift velocity. For isotropic turbulent diffusion, the diffusion coefficient $E_T$ can be related to the magnitude of $V'$ by the random walk analysis (Fischer et al. 1979), where

* 1 cp = $1.0\times10^2$ g/cm-s = 2.4 lb/ft-hr.

$$V' = (4E_T/\delta t)^{1/2} \tag{27}$$

where $\delta t$ is a time step.

Murray (1972), using the Fickian diffusion theory, estimated the value of the diffusion coefficient for the 1970 Chevron spill to be 19 $m^2/s$. Cole et al. (1973) used a value of 4.5 $ft^2/s$, based on dye tests for the simulation of an oil spill at the Cherry Point Refinery in the Strait of Georgia. Hunter (1980), by fitting observed spreading of oil slicks to Okubo's (1962) theory, suggested a value of a 5 $m^2/s$. All of these analyses were based on coastal oil spills. In rivers and shallow lakes the diffusivity will be affected by the shear velocity $u_*$ and the depth of flow $D$, in addition to the wind. Flume experiments by Sayre and Chang (1969) indicated that $E_T$ is on the order of 0.6 $Du_*$. This expression may be used to calculate turbulent diffusion in rivers. For lakes the following formula for surface dye patches (Okubo 1962) may be used:

$$E_T = 0.0027\, t^{1.34} \tag{28}$$

where $E_T$ is in $cm^2/s$ and $t$ is in seconds.

In the present simulation the fluctuation velocity component $\vec{V}'$ is calculated by

$$\vec{V}' = V' r_n e^{i\theta'}. \tag{29}$$

For a selected $E_T$ value the magnitude of $V'$ is computed using eq 27. The variable $r_n$ is a normally distributed random number with a mean value of 0 and a standard deviation of 1. The directional angle $\theta'$ is assumed to be a uniformly distributed random angle ranging between 0 and $\pi$.

During each time step $\Delta t$, the displacement $\Delta S$ of each oil parcel is calculated by numerically integrating the drift velocity $\vec{V}_t$ over the time period $\Delta t$. For numerical accuracy, when the $\Delta t$ value is large, subintervals $\delta t_k$ are used for the advection of oil parcels. In this case the displacement during the time interval $\Delta t$ is

$$\Delta\vec{S} = \sum^{k} \vec{V}_k\, \delta t_k \tag{30}$$

where $\vec{V}_k$ = drift velocity of an oil parcel during the time interval $\delta t_k$

$\Delta\vec{S}$ = displacement during the time interval $\Delta t$

$\sum^{k} \delta t_k = \Delta t$.

The values of $\delta t_k$ should satisfy the condition (Roache 1972, Cheng et al. 1984)

$$\delta t_k \le \left(\frac{u_k}{\Delta x} + \frac{v_k}{\Delta y}\right)^{-1} \tag{31}$$

where $u_k$ and $v_k$ are the $x$ and $y$ components of the velocity $V_k$.

**Mechanical spreading**

*Spreading in open water*

Spreading of the oil slick is one of the most important processes in the early stage of the oil slick transformation, because of the influence of the surface area of the oil slick on weathering processes such as evaporation and dissolution. Besides the horizontal dispersion due to advection and turbulent diffusion, the spreading of an oil slick is determined by the balance of gravitational, viscous and surface tension forces. Spreading is also affected by weathering processes, which tend to change the mass and physical–chemical properties of the slick. Several models have been proposed for the process of mechanical spreading in open water (Blokker 1964, Fay 1969, 1971, Hoult 1972, Mackay et al. 1980). In this study, Fay's spreading theory (1971) is used because this theory is based on a comprehensive description of the spreading mechanisms and has been verified by laboratory experiments (Hoult and Suchon 1970, Fay 1971) and other analytical solutions (Fannelop and Waldman 1972).

**Table 2. Spreading laws for oil slicks (Fay 1971, Hoult 1972, Waldman et al. 1973).**

| *Spreading phase* | $L_e$ *(one-dimensional)* | $R_e$ *(radial)* |
|---|---|---|
| Gravity–inertia | $1.39(\Delta g A t^2)^{1/3}$ | $1.14(\Delta g \mathcal{V} t^2)^{1/4}$ |
| Gravity–viscous | $1.39(\Delta g A^2 t^{3/2} \nu^{-1/2})^{1/4}$ | $0.98(\Delta g \mathcal{V}^2 t^{3/2} \nu^{-1/2})^{1/6}$ |
| Surface tension–viscous | $1.43\left(\sigma^2 t^3 \rho_w^{-2} \nu^{-1}\right)^{1/4}$ | $1.60\left(\sigma^2 t^3 \rho_w^{-2} \nu^{-1}\right)^{1/4}$ |

$\Delta = 1 - (\rho_o/\rho_w)$
$\nu$ = $\nu$ of water
$A$ = 0.5 volume of oil / unit length of oil slick
$\mathcal{V}$ = volume of oil slick.

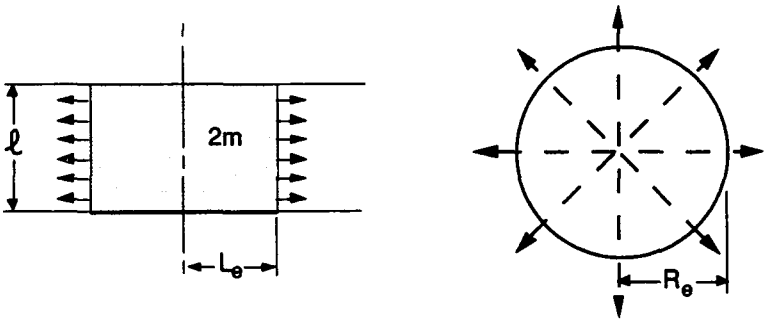


*a. One-dimensional spreading.* *b. Axisymmetric spreading.*

*Figure 8. Definition sketches for the spreading laws for oil slicks.*

Fay's spreading theory is derived for single-component, constant-volume slicks with idealized configurations in quiescent water. This theory considers the spreading of oil to be a result of two driving forces—gravity and surface tension—interbalanced by the retarding forces of inertia and viscosity. The spreading of an oil slick is considered to pass through three phases. In the beginning phase, only gravity and inertia forces are important. In the intermediate phase the gravity and viscous forces dominate. In the final phase the surface tension is balanced by viscous forces. Formulas for one-dimensional spreading and radial spreading at different stages are summarized in Table 2 using terms defined in Figure 8.

The spreading rate during each phase can be obtained by taking time derivatives of the formulas given in Table 2. The equations for spreading rates are summarized in Table 3.

**Table 3. Spreading rates of oil slicks and phase transition times.**

**A. Spreading rates for one-dimensional slicks, $dL_e/dt$.**

| *Spreading phase* | *Spreading rate* |
|---|---|
| Gravity–inertia | $(\Delta g)^{1/3}\,[L^{-1/3}(dL/dt)\,t^{2/3} + L^{2/3}\,t^{-1/3}]$ |
| Gravity–viscous | $1.39(\Delta g \nu^{-1/2})^{1/4}\,[\frac{3}{8}\,L\,t^{-5/8} + (dL/dt)\,t^{3/8}]$ |
| Surface tension–viscous | $1.43(\sigma \rho_w^{-1})^{1/2}\,(\frac{3}{4}\,t\,\nu)^{-1/4}$ |

**B. Spreading rates for circular oil slicks, $dR_e/dt$.**

| *Spreading phase* | *Spreading rate* |
|---|---|
| Gravity–inertia | $0.285(\Delta g)^{1/4}\,(t^{1/2}\,\mathcal{V}^{-3/4})\,[(d\mathcal{V}/dt) + (2\mathcal{V}/t)]$ |
| Gravity–viscous | $0.98(\Delta g \nu^{-1/2})^{1/6}\,[\frac{1}{3}\,\mathcal{V}^{-2/3}\,t^{1/4}\,(d\mathcal{V}/dt) + \frac{1}{4}\,\mathcal{V}^{1/3}\,t^{-3/4}]$ |
| Surface tension–viscous | $1.20\left(\sigma^2 \rho_w^{-1} \nu^{-1} t^{-1}\right)^{1/4}$ |

**C. Times of phase transition**

| *Transition* | *One-dimensional spreading* | *Radial spreading* |
|---|---|---|
| Gravity–inertia to gravity–viscous | $(L^9\,\nu^{-3}\,\Delta^{-2}\,g^{-2})^{1/7}$ | $0.55(\mathcal{V}\nu^{-1}\,\Delta^{-1}\,g^{-1})^{1/3}$ |
| Gravity–viscous to surface tension–viscous | $(0.89 \Delta g L^4\,\sigma^{-2}\,\rho_w^{\,2}\,\nu^{1/2})^{2/3}$ | $0.38(\rho_w/\sigma)(\Delta g \nu \mathcal{V}^2)^{1/3}$ |

$L^2$ = volume of oil per unit length along the major axis of the slick ($L$ is a characteristic length)
$\mathcal{V}$ = total volume of the slick.

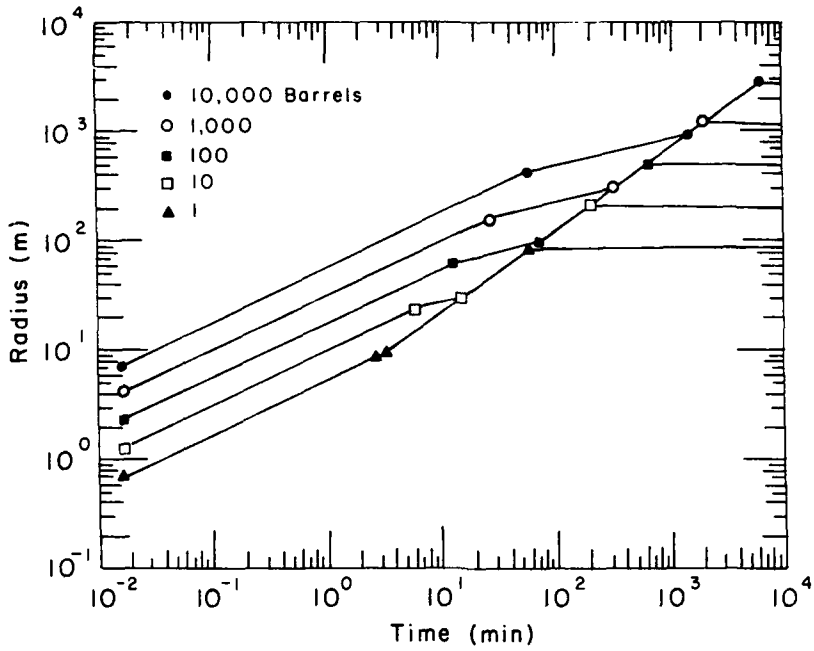


*Figure 9. Slick radius vs time ($\rho_w = 1.09\ g/cm^3$, $\rho_o = 0.9\ g/cm^3$, $\nu_w = 2.543\times 10^{-2}\ cm^2/s$, $\sigma = 11.02$ dynes/cm). The points represent phase transitions.*

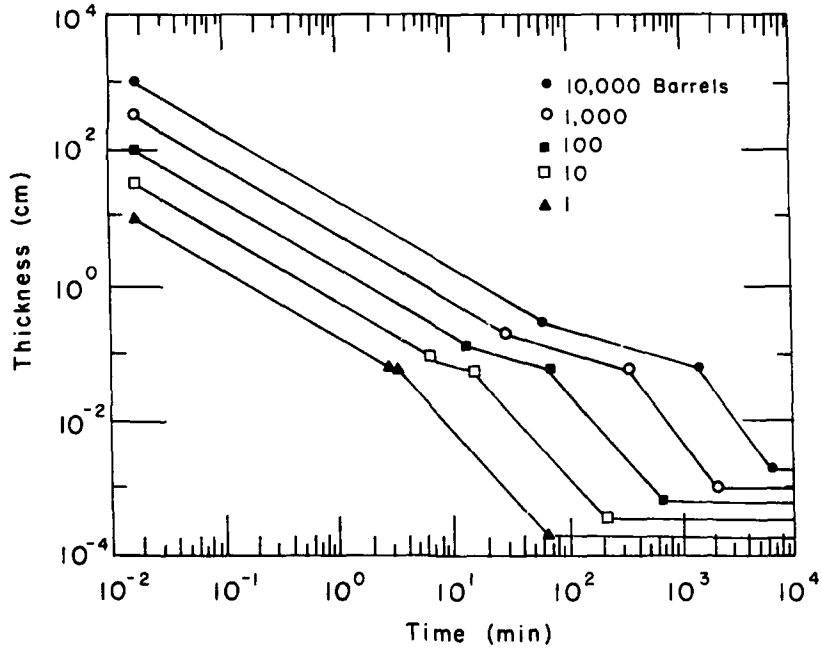


*Figure 10. Slick thickness vs time ($\rho_w = 1.09\ g/cm^3$, $\rho_o = 0.9\ g/cm^3$, $\nu_w = 2.543\times 10^{-2}\ cm^2/s$, $\sigma = 11.02$ dynes/cm). The points represent phase transitions.*

The rate of change of the oil volume in these equations represents the change due to weathering and the changes in oil volume distribution in various parts of the slick. In addition to the rates of spreading at different phases, the times at which each phase transition occurs also need to be determined. These transition times can be obtained by letting equations in the appropriate phases equal each other and solving for time. Equations for the transition times are summarized in Table 3. Fay (1969, 1971)

observed that the changes in slick properties caused by weathering may result in the eventual cessation of mechanical spreading. Based on a number of field observations, Fay suggested that

$$A_f = 10^5 \forall^{3/4} \tag{32}$$

where $A_f$ is the final slick area in $m^2$ and $\forall$ is the total volume of the slick in $m^3$. In this study the mechanical spreading is considered to cease when the slick thickness reduces to $10^{-5} \forall^{1/4}$ m. To illustrate the respective regimes of the different phases of spreading, variations of the radius and thickness of circular slicks of different volumes resulting from an instantaneous spill are presented in Figures 9 and 10.

The formulas in Tables 2 and 3 were derived for simple slick geometries that exist under idealized conditions. In the simulation model the radial spreading formulas are used when the slick is nearly circular, and the one-dimensional formulas are used when the slick area is elongated. A slick is considered to be elongated when the aspect ratio of the slick area is greater than 3. The aspect ratio refers to the length-to-width proportion of the slick, and the orientation refers to the angle $\theta$ between the major axis of the slick and the x axis, as shown in Figure 11.

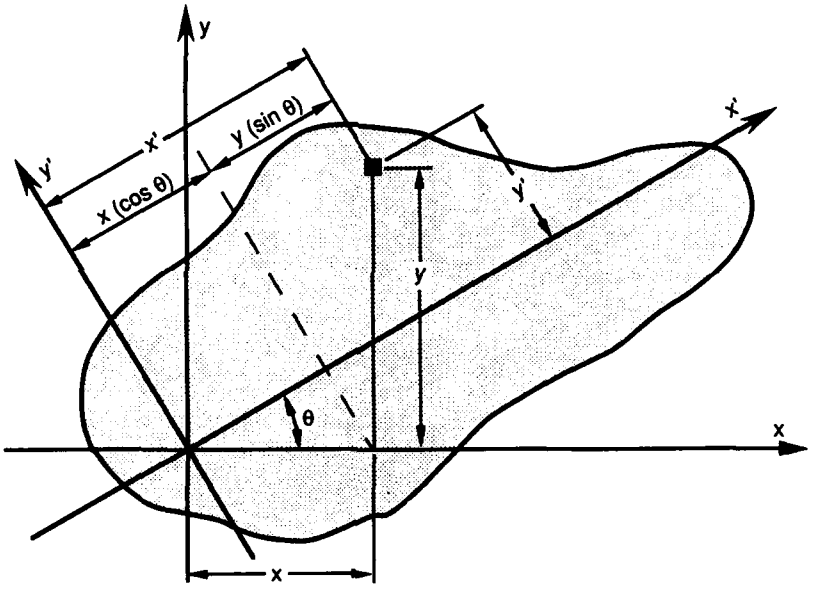


*Figure 11. Definition sketch for variables used to compute slick aspect ratio and orientation.*

The orientation of the slick is computed using the moments and product of inertia of the slick. The angle $\theta$ can be expressed using

$$\tan(2\theta) = \frac{-2P_{xy}}{I_x - I_y} \tag{33}$$

where

$$I_x = \Sigma y^2, \quad I_y = \Sigma x^2, \quad P_{xy} = \Sigma xy \tag{34}$$

where $I_x$ and $I_y$ are the moments of inertia of the oil slick with respect to the x and y axis, respectively, and $P_{xy}$ is the product of inertia. Once the orientation is known, the x and y coordinates of all the particles in the slick are transformed into coordinates in an x', y' coordinate system in which the x'

axis is the major axis of the slick. The aspect ratio is computed by eq 35 based on the x', y' coordinates of all the oil particles:

$$\text{Aspect ratio} = \frac{\Sigma x'}{\Sigma y'}. \qquad (35)$$

This aspect ratio is used to determine whether the spreading of the oil slick is radial or one-dimensional. The use of an aspect ratio of 3.0 for the transition from radial spreading to one-dimensional spreading is subjective, but it gives reasonable results.

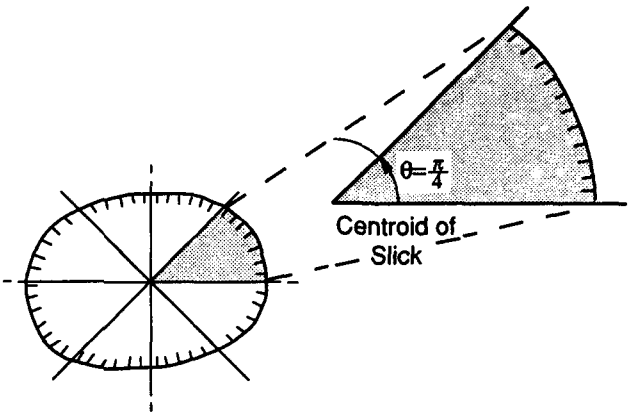


*Figure 12. Division of a nearly circular slick into pie segments.*

For a nearly circular slick the slick area is divided into eight pie-shaped sectors as shown in Figure 12. For an elongated slick the entire slick is broken up into a series of strips as shown in Figure 13. For both cases the spreading rate of each segment is calculated using Fay's formula independent of other segments in the slick. This simplification assumes that concentration gradients at the boundaries between neighboring segments are negligible for mechanical spreading. The segmentization also allows for different spreading rates in different regions of the slick, providing a more realistic description of the field situation. During each time step the increase in mean radius of each pie-shaped sector in a nearly circular slick or the mean width of each segment in an elongated slick can be calculated from the spreading formulas in Table 2.

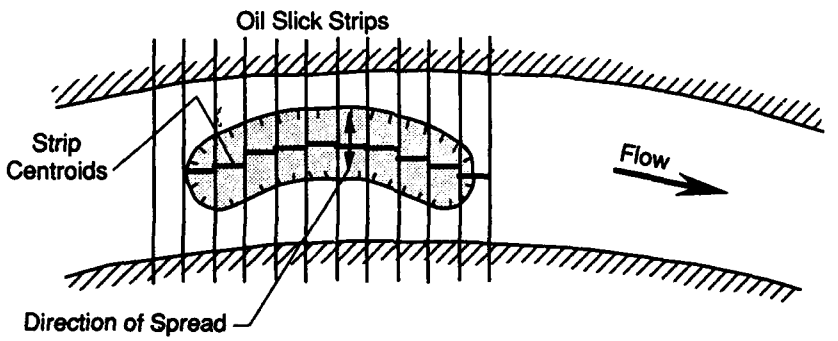


*Figure 13. Division of an elongated slick into strips.*

For a nearly circular slick the rate of outward movement of an oil parcel along the radial direction in a particular pie-shaped sector located at a distance $r$ from the centroid of the slick can be calculated from the spreading rate of the mean radius of the sector as $(r/\bar{r})(d\bar{r}/dt)$. Parcels far away from the main slick will be excluded from this process since small isolated patches of oil will not be subjected to mechanical spreading. In this study, parcels that account for the outer 5% of the total slick volume are excluded from the mechanical spreading analysis. This is equivalent to excluding the parcels located at a radial distance greater than 2.2 $r$ from the centroid of the slick. This was determined from numerical experiments for the spreading of circular slicks in a wide rectangular channel.

For an elongated slick the rate of outward movement in the width direction of an oil parcel in a segment with mean length $\bar{l}$, located a distance $l$ from the centroid of the segment, can be calculated from the rate of spreading of the mean length of the segment as $(l/\bar{l})(d\bar{l}/dt)$.

*Spreading under an ice cover*

The spreading of oil under ice covers has received little attention. However, the study of Hoult et al. (1975) has provided some information. Their study suggests that appreciable mechanical spreading will only occur during continuous spills. The oil thickness stabilizes when the equilibrium thickness for the flow condition is reached. There are no pressure gradients or surface tension forces to cause the oil to spread further. The oil reaches an equilibrium state in which cavities formed by the ice roughness contain a volume of oil that can decrease only with a significant increase in the current speed. Since a continuous spill will repeatedly add oil to fill the cavities, the excess oil will effectively spread to the empty neighboring cavities and establish an equilibrium state there. This is a crude but reasonable assessment, since only the excess oil, from overfilling the cavities under the ice cover, would be expected to spread.

The formula used to model mechanical spreading for a continuous spill under ice is

$$r = 0.25\left(\frac{\Delta g Q^2}{h'}\right)^{1/6} t^{2/3} \tag{36}$$

where $r$ = slick radius
$\Delta = (\rho_w - \rho_o)/\rho_w$, the relative density ratio
$g$ = acceleration due to gravity
$Q$ = average volume flow rate since the beginning of the spill
$h'$ = half of the root-mean-square roughness height of the ice cover.

This equation is a result of balancing the frictional drag from the ice cover with the pressure drop that occurs as the oil flows into open cavities. In the simulation models no mechanical spreading will occur for an instantaneous spill or once the continuous oil discharge stops. If the oil discharge is in progress and the slick is nearly circular, the mechanical spreading will be calculated by eq 36.

**Shoreline boundary conditions**

An oil slick will reach a shoreline sometime after a spill occurs. Gundlach and Hayes (1978) proposed a method for classifying shorelines according to their "vulnerability,"* which is an index reflecting the environmental sensitivity of the shoreline to oil pollution. For beaches of different vulnerabilities Torgrimson (1974) suggested the use of "half-life" values to describe the ability of the shore to retain the oil. Half-life describes the "absorbancy" of the shoreline by describing the rate of re-entrainment of oil after it has landed. Table 4 presents the half-lives for different types of shorelines along with their vulnerability indices.

**Table 4. Shoreline descriptor and default parameters. (After Torgrimson 1974.)**

| *Shoreline descriptor* | *Half life* | *Vulnerability index* |
|---|---|---|
| Exposed headland | 1 hour | 1 |
| Wave-cut platform | 1 hour | 2 |
| Pocket beach | 1 day | 3 |
| Sand beach | 1 day | 4 |
| Sand and gravel beach | 1 day | 5 |
| Sand and cobble beach | 1 year | 6 |
| Exposed tide flats | 1 hour | 7 |
| Sheltered rock shore | 1 year | 8 |
| Sheltered tide flat | 1 year | 9 |
| Sheltered marsh | 1 year | 10 |
| Land | 1 year | 0 |

The present model uses the half-life concept. The volume of oil remaining on the beach is related to its original volume by

$$\mathcal{V}_2 = \mathcal{V}_1 \exp\left[-k(t_2 - t_1)\right] \tag{37}$$

where $\mathcal{V}_1$ and $\mathcal{V}_2$ are the volumes of oil on the beach at times $t_1$ and $t_2$, respectively, and $k$ is a decay constant. Since during one half-life the volume of the oil on the

*For some shorelines in the United States, Environmental Sensitivity Index maps indicating types of shoreline characteristics are available. Maps for the Detroit–St. Clair river system are expected in the near future (T. Kaiser, NOAA, Ann Arbor, Michigan). This information can be used with the current model.

beach will be reduced by half, the decay constant $k$ can be expressed in terms of the half-life $\lambda$ as

$$k = [-\ln(1/2)]/\lambda . \tag{38}$$

The fraction of the oil re-entrained into the water body during each time step is

$$(V_1 - V_2)/V_1 = 1 - e^{-k\Delta t} = 1 - 0.5^{\Delta t/\lambda}. \tag{39}$$

**Evaporation**

Evaporation can account for the largest loss in oil volume during the early stage of the slick transformation. In this study the formulation developed by Mackay et al. (1980) is used to calculate the evaporation rate of the oil. The volume fraction of oil evaporated is determined as

$$F = (1/C)\,[\ln P_o + \ln(C\,K_E t + 1/P_o)] \tag{40}$$

where $E = K_E t$ = "evaporative exposure" term, which varies with time and environmental conditions

$K_E = K_M A v/(RTV_o)$

$K_M$ = mass transfer coefficient (m/s), $0.0025 U_{wind}^{0.78}$

$A$ = spill area ($m^2$)

$v$ = molar volume ($m^3$/mole)

$R$ = gas constant ($82\times10^{-6}$ atm $m^3$/(mol-K)

$T$ = surface temperature of the oil (K), which is generally close to the ambient air temperature $T_E$

$V_o$ = initial spill volume ($m^3$)

$U_{wind}$ = wind speed at 10 m above the water surface (m/s).

The initial vapor pressure $P_o$ in atmospheres at the temperature $T_E$ is

$$\ln P_o = 10.6[1 - (T_o/T_E)] \tag{41}$$

where $T_o$ is the initial boiling point (K) and $T_E$ is the ambient air temperature (K). The constant C can be determined by the relationship $T_E C$ = constant. C values for $T_E$ = 283 K and the initial boiling point $T_o$ are given in Table 5. For crude oils of different API index values, C values at $T_E$ = 283 K are given in Table 6, along with $T_o$. This table can be replaced by the following functional relationships obtained through curve fitting as shown in Figures 14 and 15:

**Table 5. Suggested evaporation parameters for various petroleum fractions ($T_E$ = 283 K). (After Mackay et al. 1980.)**

| | $T_o$ (K) | C | $P_o$ (atm) |
|---|---|---|---|
| Motor gasoline | | | |
| Summer | 314 | 5.99 | 0.313 |
| Winter | 308 | 6.23 | 0.39 |
| Aviation gasoline | 341 | 2.81 | 0.12 |
| Diesel fuel | 496 | 5.57 | $3.4\times10^{-4}$ |
| Jet fuel | 418 | 5.06 | $6.0\times10^{-3}$ |
| No. 2 furnace oil | 465 | 7.88 | $1.1\times10^{-3}$ |
| Lube (heavy and light) | 583 | 8.61 | $1.32\times10^{-3}$ |
| Heavy gas oil | 633 | 8.99 | $2.0\times10^{-6}$ |
| Residuals | 783 | 3.37 | $7.35\times10^{-9}$ |
| Light gas oil | 473 | 6.37 | $8.1\times10^{-4}$ |

**Table 6. Suggested evaporation parameters for various crude oils ($T_E$ = 283 K). (After Mackay et al. 1980.)**

| API | Specific gravity ($g/cm^3$) | C | $T_o$ (K) | $P_o$ (atm) |
|---|---|---|---|---|
| 10 | 1.0 | 89.2 | 366 | 0.044 |
| 12 | 0.986 | 69.4 | 348 | 0.088 |
| 15 | 0.966 | 52.1 | 339 | 0.13 |
| 20 | 0.934 | 34.7 | 329 | 0.18 |
| 25 | 0.904 | 27.2 | 330 | 0.17 |
| 30 | 0.876 | 22.33 | 325 | 0.21 |
| 35 | 0.850 | 19.5 | 314 | 0.31 |
| 40 | 0.825 | 17.9 | 304 | 0.45 |
| 45 | 0.802 | 16.4 | 283 | 1.004 |

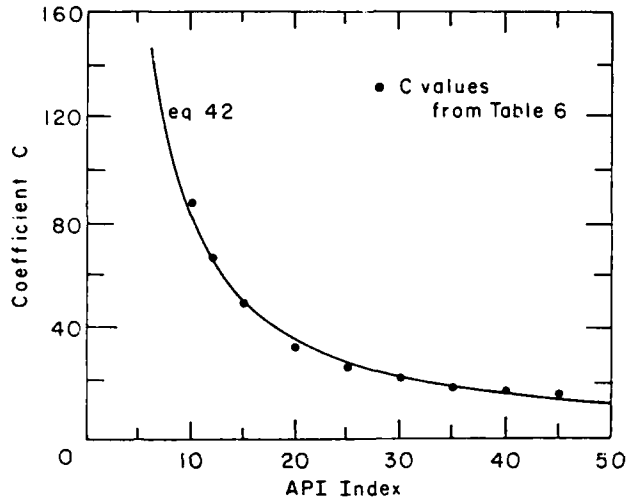


*Figure 14. Comparison of eq 42 with C values from Table 6.*

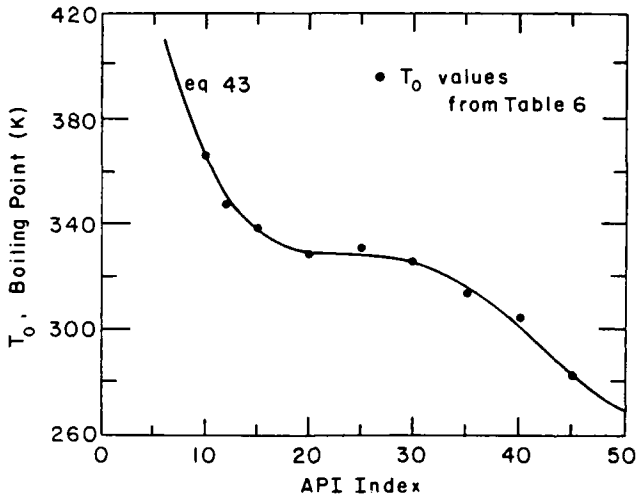


*Figure 15. Comparison of eq 43 with $T_0$ values from Table 6.*

$$C = 1158.9\ \mathrm{API}^{-1.1435} \tag{42}$$

and

$$T_o = 542.6 - 30.275\mathrm{API} + 1.565\mathrm{API}^2 - 34.39\mathrm{API}^3 + 0.0002604\mathrm{API}^4 . \tag{43}$$

The API index and the specific gravity of the oil are related by

$$\text{Specific gravity} = 141.5 / (\mathrm{API} + 131.5) . \tag{44}$$

The molar volume of oil, which is required in eq 40, can vary between $150\times10^{-6}$ and $600\times10^{-6}$ $m^3$/mole, depending on the composition of the oil. For fuel oils this value is approximately $200\times10^{-6}$ $m^3$/mole. The molar volume can be computed from the molecular weight of the oil. Typical molecular weights for various oil components are given in Table 7. Tables 7 and 8 show the compositions of several different oils, along with the molecular weight $M_i$ of each component. Based on these, the molecular volume can be computed from

$$v = 1/\Sigma(c_i M_i) \tag{45}$$

where $c_i$ is the weight of the $i$th component per unit volume of oil.

**Table 7. Basic data for oil weathering. (After Moore et al. 1973.)**

| *Fraction* | *Description* | *% by wt in crude oil* | *Density (g/mL)* | *Boiling point (°C)* | *Molecular weight* | *Vapor pressure at 20°C (mm)* | *Solubility ($g/10^6$ g distilled $H_2O$)* |
|---|---|---|---|---|---|---|---|
| 1 | Paraffins ($C_6$–$C_{12}$) | 0.1–20 | 0.66–0.77 | 69–230 | 86–170 | 110–0.1 | 9.5–0.01 |
| 2 | Paraffins ($C_{13}$–$C_{25}$) | 0–10 | 0.77–0.78 | 230–405 | 184–352 | 0.1 | 0.01–0.004 |
| 3 | Cycloparaffins ($C_6$–$C_{12}$) | 5–30 | 0.75–0.9 | 70–230 | 84–164 | 100–1.0 | 55–1.0 |
| 4 | Cycloparaffins ($C_{13}$–$C_{23}$) | 5–30 | 0.9–1.0 | 230–405 | 156–318 | 1.0–0 | 1.0–0 |
| 5 | Mono- and di-cyclic aromatics ($C_6$–$C_{11}$) | 0–5 | 0.88–1.1 | 80–240 | 78–143 | 72–0.1 | 1780–0 |
| 6 | Polycyclic aromatics ($C_{12}$–$C_{18}$) | 0–5 | 1.1–1.2 | 240–400 | 128–234 | 0.1–0 | 12.5–0 |
| 7 | Naphtheno-aromatics ($C_9$–$C_{25}$) | 5–30 | 0.97–1.2 | 180–400 | 116–300 | 1.0–0 | 1.0–0 |
| 8 | Residual (including heterocycles) | 10–70 | 1.0–1.1 | > 400 | 300–900 | 0 | 0 |

**Table 8. Estimated composition and comparison of solubilities for various petroleum substances. (After Moore et al. 1973.)**

| | | *Composition (% by weight)* | | | | |
|---|---|---|---|---|---|---|
| *Fraction* | *Description* | *Crude A* | *Crude B* | *# 2 fuel oil* | *Kerosene* | *Bunker C* |
| 1 | Alkanes ($C_6$–$C_{12}$) | 1 | 10 | 15 | 15 | 0 |
| 2 | Alkanes ($C_{13}$–$C_{25}$) | 1 | 7 | 20 | 20 | 1 |
| 3 | Cycloparaffins($C_6$–$C_{12}$) | 5 | 15 | 15 | 20 | 0 |
| 4 | Cycloparaffins ($C_{13}$–$C_{25}$) | 5 | 20 | 15 | 20 | 1 |
| 5 | Mono- and di-cyclic aromatics ($C_6$–$C_{11}$) | 2 | 5 | 15 | 15 | 0 |
| 6 | Polycyclic aromatics ($C_{12}$–$C_{18}$) | 6 | 3 | 5 | 2 | 1 |
| 7 | Naphtheno-aromatics ($C_9$–$C_{25}$) | 15 | 15 | 15 | 8 | 1 |
| 8 | Residual | 65 | 25 | — | — | 96 |

## Dissolution

Dissolution is an important process from the point of view of possible biological harm, although it accounts for a negligible fraction of the mass balance of the oil. Hydrocarbons that are likely to dissolve in the water are also likely to evaporate. Dissolution, which tends to occur in the first few hours of a spill, thus competes with evaporation. Although solubility values for various hydrocarbon components are available, these values are difficult to use correctly for modeling purposes since they are often inconsistent for the same compounds.

The present study uses the method of Cohen et al. (1980). In this method the total dissolution rate $N$ is calculated by

$$N = K A_s S \tag{46}$$

where $N$ = total dissolution rate of the slick (g/hr)
$K$ = dissolution mass transfer coefficient, assumed to be 0.01 m/hr
$A_s$ = slick area ($m^2$)
$S$ = oil solubility in water.

Huang and Montastero (1982) suggested that the solubility for a typical oil can be calculated by

$$S = S_o e^{-0.1t} \tag{47}$$

where $S_o$ is the solubility for fresh oil and $t$ is the time in hours. Huang and Monastero suggested a typical value of 30 g/$m^3$ for $S_o$. The study of Lu and Polak (1973) provided more information on solubility; they formulated the rate of dissolution as

$$r_d = cd\, e^{-dt} \tag{48}$$

where $r_d$ is the rate of dissolution (mg $m^2$/day). For three oil samples tested, the coefficients $c$ and $d$ are shown in Table 9.

**Table 9. Dissolution coefficients at 25°C. (After Lu and Polak 1973.)**

| *Oil type* | *API* | *c* *(mg/m²)* | *d* *(day⁻¹)* | $KS_o = cd$ *(gm⁻² hr⁻¹)* |
|---|---|---|---|---|
| No. 2 fuel oil | 35.5 | 1043 | 0.423 | 0.0184 |
| Crude oil | 38.6 | 8915 | 2.380 | 0.884 |
| Bunker C oil | 14.8 | 459 | 0.503 | 0.0104 |

## MODEL APPLICATIONS

Based on the analytical formulation, two computer models were developed and applied to the connecting channels of the upper Great Lakes. These two models are named ROSS (River Oil Spill Simulation) and LROSS (Lake and River Oil Spill Simulation). ROSS was developed for simulating oil spills in rivers and was applied to the Detroit River, St. Clair River, lower St. Marys River and upper St. Marys River. LROSS was developed for simulating oil spills in lake–river systems and was applied to the Lake St. Clair–Detroit River system. The details of the model structure, instructions for input data preparation, sample output and program listing for both models are given in the user's manuals (Shen et al., in prep. a,b, Yapa et al., in prep.).

To illustrate the applicability of the computer models, three sample simulations are presented here (Fig. 16–18). In all three cases no. 2 fuel oil, with a specific gravity of 0.84 and a surface tension of 30 dynes/cm, was selected as the spill material. The other input parameters for each case are summarized in Table 10. The evaporation characteristics used are $T_o$ = 465 K, $C$ = 7.88 and $v = 2\times10^{-4}$ $m^3$/mole. The solubility of the oil was assumed to be $0.1873\times10^2$ lb/$ft^3$. A time step of 15 minutes was used in all three simulations.

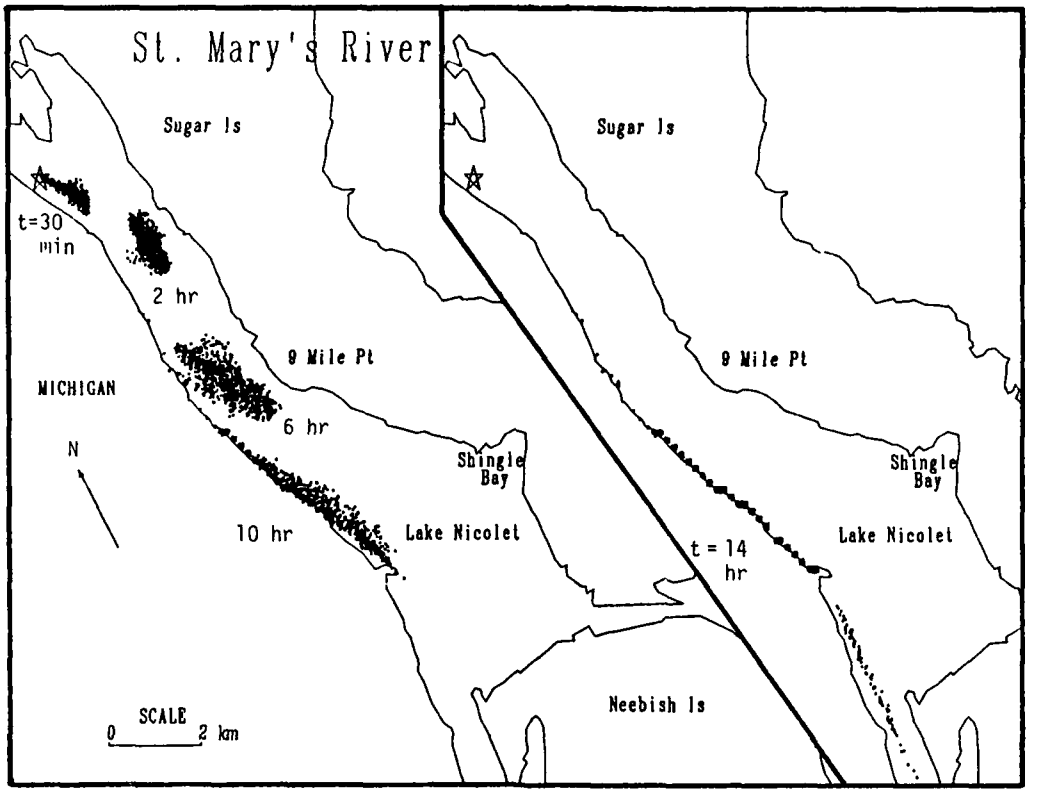


*Figure 16. Result of a sample simulation of oil slick transformation in the lower St. Marys River.*

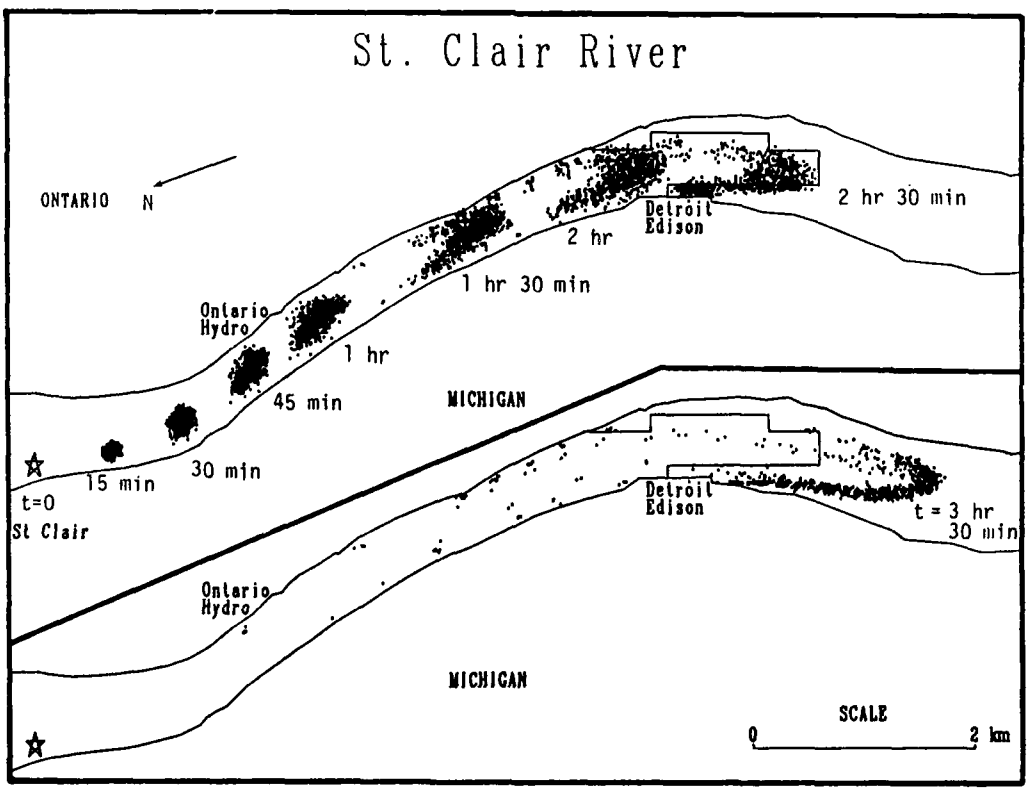


*Figure 17. Result of a sample simulation of oil slick transformation in the St. Clair River.*

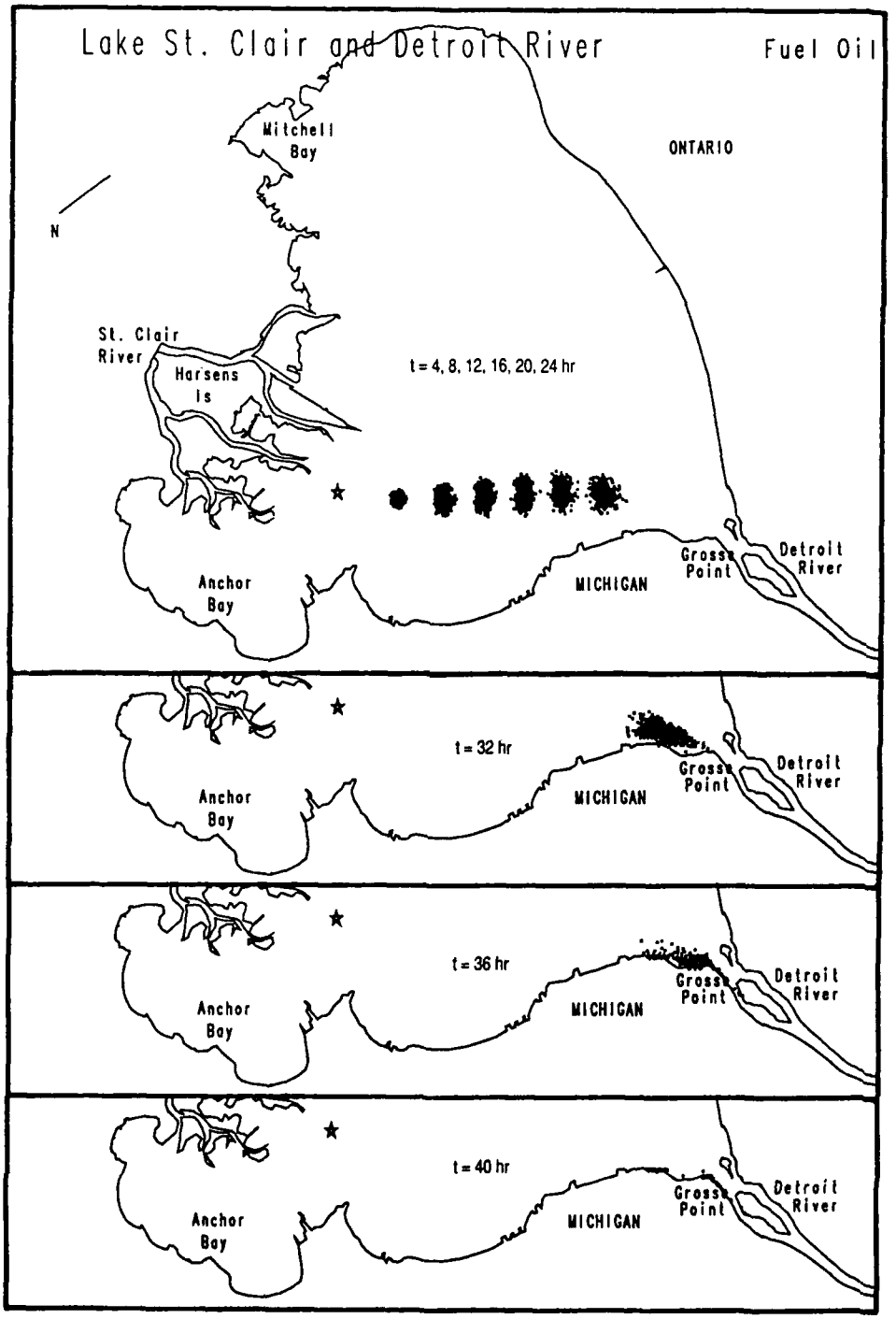


*Figure 18. Result of a sample simulation of oil slick transformation in the Lake St. Clair–Detroit River system.*

**Table 10. Model input parameters for sample simulations.**

| | *Case 1* | *Case 2* | *Case 3* |
|---|---|---|---|
| Spill location | Lower St. Marys River | St. Clair River near Frechette Point | Lake St. Clair near St. Clair |
| Spill type | Continuous leak, duration = 30 min. | Instantaneous spill | Instantaneous spill |
| Spill volume | 35,000 L (9,247 gal.) | 19,000 L (5,020 gal.) | 37,850 L (10,000 gal.) |
| Oil type | No. 2 fuel oil (sp. gr. = 0.84) | Crude oil (sp. gr. = 0.86) | No. 2 fuel oil (sp. gr. = 0.84) |
| Flow conditions | Discharge = 111,017 $ft^3/s$; water level at downstream side of Soo Locks = 581.40ft | Discharge = 130,000 $ft^3/s$; water level at upstream side of St. Clair River = 575.00 ft | Discharge = 210,000 $ft^3/s$; water level at lake outlet = 575.04 ft |
| Ice conditions | Open water | Partially covered downstream of Detroit Edison with 15-cm ice cover, $n_i$ = 0.035 | Open water |
| Wind conditions | 0–3 hr: 6.6 mph from W<br>3–6 hr: 6.6 mph from E<br>6–14 hr: 9.8 mph from N | 0–3.5 hr: 1.3 mph from W | 0–24 hr: 10 mph from NE<br>24–40 hr: 2 mph from E |
| Diffusion coefficient (Du.) | 0.6 | 0.6 | — |
| Air temperature (°F) | 50 | 20 | 50 |
| Water viscosity ($m^2/s$) | $1.308 \times 10^{-6}$ | $1.792 \times 10^{-6}$ | $1.308 \times 10^{-6}$ |
| Oil viscosity (poise) | — | 0.158 | — |
| Surface tension (dyne/cm) | 30 | 30 | 30 |
| Evaporation parameters | | | |
| $T_o$ (K) | 465 | 321 | 465 |
| $C$ | 7.88 | 21.3 | 7.88 |
| Solubility parameters | | | |
| $kS_o$ ($g^{-2}hr^{-1}$) | 0.0184 | 0.884 | 0.0184 |
| $\alpha$ ($day^{-1}$) | 0.423 | 2.380 | 0.423 |

## SUMMARY AND CONCLUSIONS

In this study, two-dimensional computer models for simulating oil slick movement in rivers and lakes were developed. The models were then applied to the connecting channels of the upper Great Lakes. In these models the oil slick is considered to be a collection of discrete oil patches. The transformation of an oil slick due to advection, spreading, evaporation and dissolution are considered. In open-water regions the advection of oil patches in the slick are determined by the water current and wind using the drifting factor formulation. In ice-covered regions the advection of the oil is determined by an empirical formula developed by Cox and Schultz (1981). The current distribution in the lake is determined by a rigid-lid circulation model (Schwab et al. 1981). The current distribution in the river is determined by a stream-tube method. In the spreading process, mechanical spreading formulas developed by Fay (1969) and Hoult (1972) are used. These formulas consider the balance of inertia, gravity, viscous and surface tension forces. In ice-covered regions the formula developed by

Hoult et al. (1975) is used. In addition to mechanical spreading, the horizontal turbulent diffusion of the oil patches is simulated by a random-walk formulation. Formulations developed by Mackay et al. (1980) and Cohen et al. (1980) are used to determine the rate of evaporation and dissolution. Boundary conditions along the shore are formulated according to the oil retention capability of the shoreline.

The oil slick transformation model developed in this study contains as many processes as can be effectively and analytically modeled. In addition to computational efficiency, the model has several special features, including the ability to model instantaneous and continuous spills, the ability to realistically describe the irregular shapes of an oil slick and the ability to account for the time-dependent variation of the flow conditions. Improvements on parts of the model will be possible as better formulations of the oil slick transformation processes become available. The computer programs are designed so that it will be easy to refine the model elements and expand the model to include additional slick transformation processes.

## LITERATURE CITED


**Ahlstrom, S.W.** (1975) A mathematical model for predicting the transport of oil in marine waters. Battelle Pacific Northwest Laboratories, Richland, Washington.

**Argiroff, C. and L.E. Weigum** (1986) Great Lakes—Limited season extension. In *Proceedings, IAHR Ice Symposium, Iowa City, Iowa*, p. 75–86.

**Beurket, R.T. and C. Argiroff** (1984) Great Lakes limited season extension operation of Sault Ste. Marie Locks, Michigan. In *Proceedings, IAHR Ice Symposium, Hamburg, Germany*, p. 267–276.

**Bishop, P.L.** (1983) *Marine Pollution and Its Control*. New York: McGraw-Hill Book Co.

**Blokker, P.C.** (1964) Spreading and evaporation of petroleum products on water. In *Proceedings, 4th International Harbour Congress, Antwerp*, p. 911–919.

**Boyd, J.D.** (1979) A surface spill model for the Great Lakes. Contribution No. 183, Great Lakes Environmental Research Laboratory, National Oceanic and Atmospheric Administration.

**Butler, J., J. Morris and T. Slecter** (1976) The fate of petroleum in the open ocean. In *Sources, Effects and Sinks of Hydrocarbons in the Aquatic Environment*, The American Institute of Biological Sciences, p. 287–297.

**Cheng, R.T., V. Casulli and S.N. Milford** (1984) Eulerian–Lagrangian solution of the convection–dispersion equation in natural coordinates. *Water Resources Research*, **20**(7): 944–952.

**Cohen, Y., D. MacKay and W.Y. Shiu** (1980) Mass transfer rates between oil slicks and water. *The Canadian Journal of Chemical Engineering*, vol. 58.

**Cole, C.R., H.P. Foote and J.R. Eliason** (1973) Oil spill drift forecasting model. Technical Report, Battelle Pacific Northwest Laboratories, Richland, Washington. (Also paper presented at the Fourth Joint Chemical Engineering Conference, A.I.Ch.E., Vancouver, 1973).

**Cox, J.C. and L.A. Schultz** (1981) The containment of oil spilled under rough ice. In *Proceedings of the 1981 Oil Spill Conference*. American Petroleum Institute, Washington, D.C., p. 203–208.

**DePietro, N.D. and R.G. Cox** (1979) The dynamics of spreading of oil on the surface of water. In *Workshop on the Physical Behavior of Oil in the Marine Environment, Princeton University*, p. 2.1–2.14.

**Fannelop, T.K. and G.D. Waldman** (1972) Dynamics of oil slicks. *American Institute of Aeronautics Journal*, **10**: 506–510.

**Fay, J.A.** (1969) The spread of oil slicks on a calm sea. In *Oil on the Sea* (D. Hoult, Ed.). New York: Plenum Press, p. 53–64.

**Fay, J.A.** (1971) Physical processes in the spread of oil on a water surface. In *Proceedings of the Joint Conference on Prevention and Control of Oil Spills*. Sponsored by American Petroleum Institute, Environmental Protection Agency and U.S. Coast Guard. Washington, D.C.: American Petroleum Institute, p. 463–467.

**Fischer, H.B., E.J. List, R.C.Y. Koh, J. Imberger and N.H. Brooks** (1979) *Mixing in Inland and Coastal Waters*. New York: Academic Press, p. 483.
**Fingas, M. and M. Sydor** (1980) Development of an oil spill model for the St. Lawrence River. Inland Waters Directorate, Water Management and Planning Branch, Technical Bulletin 116.
**Foda, M. and R.G. Cox** (1980) The spreading of thin liquid films on a water/air interface. *Journal of Fluid Mechanics*, **101**(Part I): 33–51.
**Grubert, J.P.** (1976) Numerical computation of two-dimensional flows. *Journal of the Waterways, Harbors and Coastal Engineering Division, ASCE*, **102**(WW1): 1–12.
**Galt, J.A. and G.M. Torgrimson** (1979) On-scene trajectory modeling for the U.S. response to the Ixtoc-I blowout. In *Proceedings of the Workshop on Government Oil Spill Modeling*. Princeton University and National Oceanic and Atmospheric Administration.
**Gundlach, E.R. and M.D. Hayes** (1978) Vulnerability of coastal environments to oil spill impacts. *Marine Technical Society Journal*, **12**(4): 18–27.
**Hamilton, G.D., C.W. Soileau and A.D. Stroud** (1982) Numerical modeling study of Lake Pontchautrain. *Journal of the Waterways, Ports, Coastal and Ocean Division, ASCE*, **108:** 49–64.
**Hoult, D.P.** (1972) Oil spreading on the sea. *Annual Review of Fluid Mechanics*, 341–367.
**Hoult, D.P. and W. Suchon** (1970) The spread of oil in a channel. Department of Mechanical Engineering, Massachusetts Institute of Technology, Cambridge, Massachusetts.
**Hoult, D.P., S. Wolfe, S. O'Dea and J.P. Patureau** (1975) Oil in the Arctic. Massachusetts Institute of Technology, Cambridge, Massachusetts, Report No. CG-D-96-75.
**Huang, J.C. and F.C. Monastero** (1982) Review of the state-of-the-art of oil spill simulation models. Final Report submitted to the American Petroleum Institute.
**Hunter, J.R.** (1980) An interactive computer model of oil slick motion. In *Proceedings, Oceanology International '80, United Kingdom*, p. 42–50.
**Jordon, R.E. and J.R. Payne** (1980) *Fate and Weathering of Petroleum Spills in the Marine Environment*. Ann Arbor, Michigan: Ann Arbor Science.
**Kerr, C. and K. Babu** (1970) The collapse of a column of fluid onto a horizontal surface. In *Proceedings of Workshop on the Physical Behavior of Oil in the Marine Environment, Princeton University*.
**Leendretse, J.J.** (1970) A water-quality simulation model for well-mixed estuaries and coastal seas. Volume I, Principles of computation. The Rand Corporation, Santa Monica, California, Report RM-6230-RC .
**Lu, C.Y. and J. Polak** (1973) A study of solubility of oil in water. Environmental Protection Service, Canada, Report EP5-4-EC-76-1.
**Mackay, D., S. Paterson and S. Nadeau** (1980) Calculation of the evaporation rate of volatile liquids. In *Proceedings, National Conference on Control of Hazardous Material Spills, Louisville, Kentucky*, p. 361–368.
**Mackay, D., S. Paterson and K. Trudel** (1980) A mathematical model of oil spill behavior. Environmental Protection Service, Fisheries and Environment Canada.
**Madsen, O.S.** (1977) A realistic model of the wind-induced Ekman boundary layer. *Journal of Physical Oceanography*, 7(N2): 248–255.
**Moore, S.F., R.L. Dwyer and A.M. Katz** (1973) A preliminary assessment of the environmental vulnerability of Machias Bay, Maine, to oil supertankers. Parsons Laboratory, MIT, Report No. 162
**Murray, S.P.** (1972) Turbulent diffusion of oil in the ocean. *Limnology and Oceanography*, **17**(5): 651–660.
**Okubo, A.** (1962) A review of theoretical models of turbulent diffusion in the sea. Chesapeake Bay Institute, The Johns Hopkins University, Technical Report 30, p. 105.
**Roache, R.J.** (1972) *Computational Fluid Dynamics*. Albuquerque, New Mexico: Hermosa Publishers.
**Rouse, H.** (1946) *Elementary Fluid Mechanics*. New York: John Wiley & Sons, Inc., p. 360.
**Sayre, W.W. and F.M. Chang** (1969) A laboratory investigation of open-channel dispersion processes for dissolved, suspended, and floating dispersants. U.S.G.S. Professional Paper 433-E, p. 71.

**Schwab, D.J., J.R. Bennet and A.T. Jessup** (1981) A two-dimensional lake circulation modeling system. Great Lakes Environmental Research Laboratory, Ann Arbor, Michigan, NOAA Technical Memorandum ERL GLERL-38.

**Schwab, D.J., J.R. Bennet and E.W. Lynn** (1984) PATHFINDER—A trajectory prediction system for the Great Lakes. Great Lakes Environmental Research Laboratory, Ann Arbor, Michigan, NOAA Technical Memorandum ERL GLERL-53.

**Schwartzberg, H.G.** (1971) The movement of oil spills. In *Proceedings, Joint Conference on Prevention and Control of Oil Spills*. American Petroleum Institute, p. 489-494.

**Shen, H.T., P.D. Yapa and M.E. Petroski** (in prep. a) Simulation of oil slick transport in Great Lakes connecting channels. User's manual for the River Oil Spill Simulation model. USA Cold Regions Research and Engineering Laboratory, Special Report.

**Shen, H.T., P.D. Yapa and M.E. Petroski** (in prep. b) Simulation of oil slick transport in Great Lakes connecting channels. User's manual for the Lake–River Oil Spill Simulation model. USA Cold Regions Research and Engineering Laboratory, Special Report.

**Shen, H.T. and N.L. Ackermann** (1980) Wintertime flow distribution in river channels. *Journal of the Hydraulics Division, ASCE*, **106**(HY5): 805–817.

**Stolzenbach, K.D., O.S. Madsen, E.E. Adams, A.M. Pollack and C.K. Cooper** (1977) A review and evaluation of basic techniques for predicting the behavior of surface oil slicks. Department of Civil Engineering, Massachusetts Institute of Technology, Cambridge, Massachusetts, Report No. 22.

**Torgrimson, G.M.** (1974) The on-scene-spill model: A user's guide. NOAA Hazardous Materials Response Branch, Technical Report (unpublished manuscript).

**Tsahalis, D.T.** (1979a) Theoretical and experimental study of wind and wave-induced drift. *Journal of Physical Oceanography*, **9**: 1243–1257.

**Tsahalis, D.T.** (1979b) Contingency planning for oil spills: RIVERSPILL—A river simulation model. In *Proceedings of the 1979 Oil Spill Conference*. Washington, D.C.: American Petroleum Institute.

**U.S. Army Corps of Engineers, Detroit District** (1974) Detroit River aerial drogue survey and mean velocity distribution study. River Current Studies, Great Lakes Hydraulics and Hydrology Branch.

**Waldman, G.A., R.A. Johnson and P.C. Smith** (1973) The spreading and transport of oil slicks on the open ocean in the presence of wind, waves, and currents. U.S. Coast Guard Report No. CG-D-17-73, AD-763 926.

**Wheeler, R.B.** (1978) The fate of petroleum in the marine environment. Exxon Production Research Company Special Report.

**Yapa, P.D., R.J. Thomas, R.S. Rutherford and H.T. Shen** (in prep.) Simulation of oil slick transport in Great Lakes connecting channels. User's manual for the microcomputer-based interactive program. U.S.A. Cold Regions Research and Engineering Laboratory, Special Report.

# REPORT DOCUMENTATION PAGE

*Form Approved*
*OMB No. 0704-0188*

Public reporting burden for this collection of information is estimated to average 1 hour per response, including the time for reviewing instructions, searching existing data sources, gathering and maintaining the data needed, and completing and reviewing the collection of information. Send comments regarding this burden estimate or any other aspect of this collection of information, including suggestion for reducing this burden, to Washington Headquarters Services, Directorate for Information Operations and Reports, 1215 Jefferson Davis Highway, Suite 1204, Arlington, VA 22202-4302, and to the Office of Management and Budget, Paperwork Reduction Project (0704-0188), Washington, DC 20503.

| 1. AGENCY USE ONLY (Leave blank) | 2. REPORT DATE | 3. REPORT TYPE AND DATES COVERED |
|---|---|---|
| | February 1990 | |

**4. TITLE AND SUBTITLE**

Simulation of Oil Slick Transport in Great Lakes Connecting Channels: Theory and Model Formulation

**5. FUNDING NUMBERS**

Contract No. DACA33-85-0001

**6. AUTHORS**

Hung Tao Shen, Poojitha D. Yapa and Mark E. Petroski

**7. PERFORMING ORGANIZATION NAME(S) AND ADDRESS(ES)**

Clarkson University
Potsdam, New York

**8. PERFORMING ORGANIZATION REPORT NUMBER**

**9. SPONSORING/MONITORING AGENCY NAME(S) AND ADDRESS(ES)**

U.S. Army Engineer District, Detroit
Detroit, Michigan 48231-1027
and
U.S.Army Cold Regions Research and Engineering Laboratory
Hanover, New Hampshire 03755-1290

**10. SPONSORING/MONITORING AGENCY REPORT NUMBER**

CRREL Report 90-1

**11. SUPPLEMENTARY NOTES**

**12a. DISTRIBUTION/AVAILABILITY STATEMENT**

Approved for public release; distribution is unlimited.

Available from NTIS, Springfield, Virginia 22161

**12b. DISTRIBUTION CODE**

**13. ABSTRACT** (*Maximum 200 words*)

The growing concern over the impacts of oil spills on aquatic environments has led to the development of many computer models for simulating the transport and spreading of oil slicks in surface water. Almost all of these models were developed for coastal environments. In this study, two computer models, named as ROSS and LROSS, were developed for simulating oil slick transport in rivers and lakes, respectively. The oil slick transformation processes considered in these models include advection, spreading, evaporation and dissolution. These models can be used for slicks of any shape originated from instantaneous or continuous spills in rivers and lakes with or without ice covers. Although the study was originated by U.S. Army Corps of Engineers, Detroit District in relation to the Great Lakes limited navigation season extension study, these models can be used for any river and lake.

**14. SUBJECT TERMS**

Computer models
Great Lakes connecting channels
Oil slicks
Oil spills

**15. NUMBER OF PAGES**
35

**16. PRICE CODE**

| 17. SECURITY CLASSIFICATION OF REPORT | 18. SECURITY CLASSIFICATION OF THIS PAGE | 19. SECURITY CLASSIFICATION OF ABSTRACT | 20. LIMITATION OF ABSTRACT |
|---|---|---|---|
| UNCLASSIFIED | UNCLASSIFIED | UNCLASSIFIED | UL |

NSN 7540-01-280-5500

☆ U. S. GOVERNMENT PRINTING OFFICE: 1990--701-136

Standard Form 298 (Rev. 2-89)
Prescribed by ANSI Std. Z39-18
298-102